

A CUT-AND-PASTE APPROACH TO CONTACT TOPOLOGY

WILLIAM H. KAZEZ



CONTENTS

1. Convex Surfaces	1
2. Preview	8
3. Convex Decompositions	9
4. Tori	19
5. Surface bundles	27
6. Open Questions	36
References	42

1. CONVEX SURFACES

Unless otherwise stated, M will denote a compact orientable 3-dimensional manifold and may have nonempty boundary.

Definition 1. A (positive) contact structure, ξ on M , is a smooth 2-plane bundle $\xi_p \subset TM$ such that there exists a 1-form α , satisfying

- (1) $\ker_p(\alpha) = \xi_p$ for all $p \in M$ and
- (2) $\alpha \wedge d\alpha > 0$.

Example 1. Figure 1 shows a family of planes in \mathbb{R}^3 that is invariant under rotation about the z -axis or translation in the z -direction. The indicated line L is Legendrian, that is, $T_x L \subset \xi_x$ for all $x \in L$. Note the planes twist slowly to the left as you move along L in either direction. This example can be made more explicit by taking ξ to be the kernel of $\alpha = rd\theta + dz$ and checking that it is a contact structure.

The next definition and many of the results in the section are due to Giroux, [18].

Date: September 26, 2002.

1991 Mathematics Subject Classification. Primary 57M50; Secondary 53C15.

Key words and phrases. tight, contact structure.

Supported in part by NSF grant DMS-0073029.

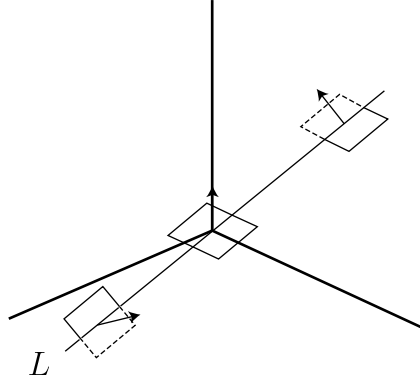
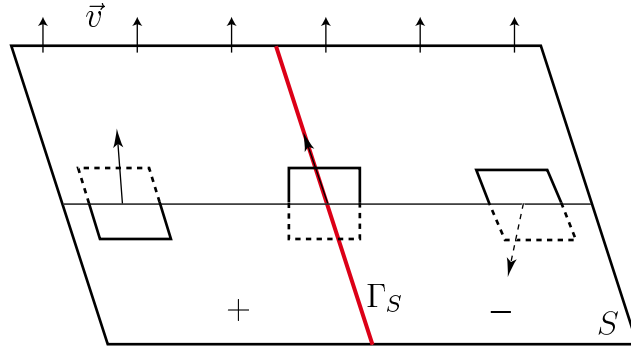
FIGURE 1. A rotationally symmetric contact structure on \mathbb{R}^3 .

FIGURE 2. Dividing curve on a convex surface.

Definition 2. A surface $S \subset (M, \xi)$ is convex if there exists vector field \vec{v} supported in a neighborhood of S and transverse to S such that flowing in the \vec{v} direction preserves the contact planes. If $\partial S \neq \emptyset$, we also require that ∂S be Legendrian. Such a \vec{v} is called a contact vector field for ξ .

Example 2. If ξ is the contact structure of Example 1, it follows that any horizontal plane is convex by considering the constant vector field $\vec{v} = \frac{\partial}{\partial z}$. Indeed it follows that any surface in \mathbb{R}^3 transverse to the vector field $\frac{\partial}{\partial z}$ is convex.

Roughly, S is convex if and only if S has a product neighborhood. Convexity is a global condition; all smooth surfaces are locally convex.

Definition 3. If $S \subset (M, \xi)$ is convex, the dividing set is denoted Γ_S and is defined to be $\{x \in S \mid \vec{v}(x) \in \xi_x\}$.

Intuition: If we think of the vector field \vec{v} as vertical or perpendicular to S , then Γ_S are those points whose contact planes are perpendicular to S .

Definition 4. The induced (singular) foliation \mathcal{F}_S on S is defined by integrating the line field $\xi_p \cap T_p S$ on S .

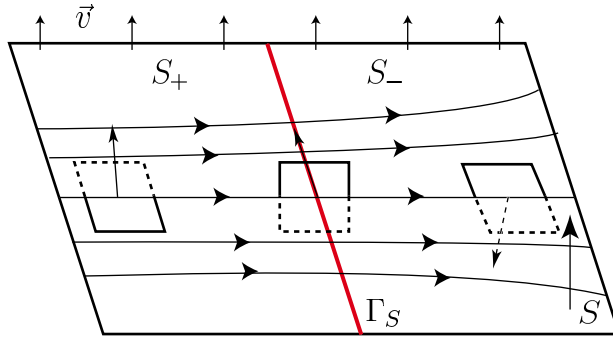


FIGURE 3. The induced foliation near a dividing curve.

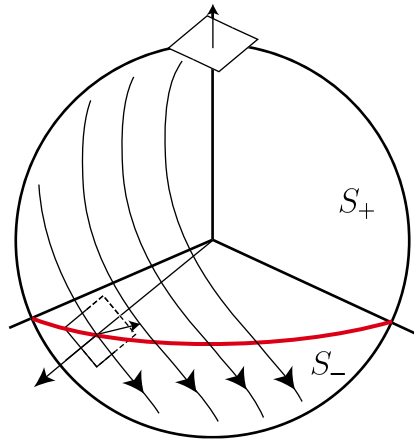


FIGURE 4. The induced foliation on a small sphere.

Throughout this paper all manifolds and submanifolds are oriented. Our contact structures are positive, thus the contact planes inherit a transverse orientation. Orientations on M , S , and ξ allow us to orient the leaves of \mathcal{F}_S . Comparing these orientations leads to two ways of thinking about dividing sets:

- (1) The dividing set Γ_S divides S into regions where the contact planes are right side up or upside down relative to S and as shown in Figure 2.
- (2) With respect to the induced foliation on S , Γ_S divides S into *source* and *sink* regions as shown in Figure 3.

Example 3. *Figure 4 shows the induced foliation and dividing set on a small round sphere about the origin of Example 1. Contact structures are locally homogeneous by Pfaff's Theorem. It follows that there exist small spheres like this about every point of any contact structure.*

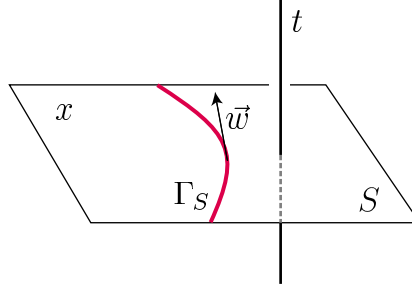


FIGURE 5. Coordinates near a convex surface.

Proposition 1. *The dividing set Γ_S is a 1-dimensional submanifold of S transverse to \mathcal{F}_S .*

Proof. Choose coordinates $x \in S$ and t in the \vec{v} direction. Then the 1-form defining ξ may be written $\alpha = \beta(x) + f(x)dt$ where $\beta(x)$ is a 1-form on S , and f is a function on S . Since $\ker \alpha = \xi$ we have:

- (1) $\alpha_x \left(\frac{\partial}{\partial t} \right) = 0$ if and only if $f(x) = 0$, and therefore $\Gamma_S = f^{-1}(0)$.
- (2) $0 \neq \alpha \wedge d\alpha = (\beta + fdt) \wedge (d\beta + dfdt) = \beta \wedge d\beta + \beta dfdt + fdt d\beta + \beta dfdt + fdt d\beta$. Therefore, if $f(x) = 0$, then $\beta dfdt \neq 0$, and in particular $df \neq 0$. It now follows that $\Gamma_S = f^{-1}(0)$ is a submanifold of S .
- (3) Let \vec{w} be tangent to Γ_S . Then $dt(\vec{w}) = df(\vec{w}) = 0$, so $\beta dfdt \neq 0$ implies that $\beta(\vec{w}) \neq 0$, that is, $\vec{w} \notin \ker \beta = T\mathcal{F}_S$. It now follows that Γ_S is transverse to the induced foliation on S .

□

The next several results will be used throughout the paper.

Proposition 2. *The isotopy class of Γ_S does not depend on the choice of the contact vector field \vec{v} .* □

Theorem 1 (Existence of convex surfaces). *Every closed surface or compact surface with Legendrian boundary can be approximated by a convex surface.*

Theorem 1 was proved by Giroux [18] for closed surfaces and by Honda for surfaces with boundary [20]. Convex surfaces with Legendrian boundary were first used by Kanda [25]. Theorem 1 follows from

Proposition 3. *If ∂S is Legendrian and the induced foliation, \mathcal{F}_S , is Morse-Smale, that is,*

- (1) \mathcal{F}_S has a finite number of closed leaves and Morse type singularities,
- (2) there are no saddle-saddle connections,
- (3) the holonomy about closed leaves is linear and either attracting or repelling,

then S is convex. □

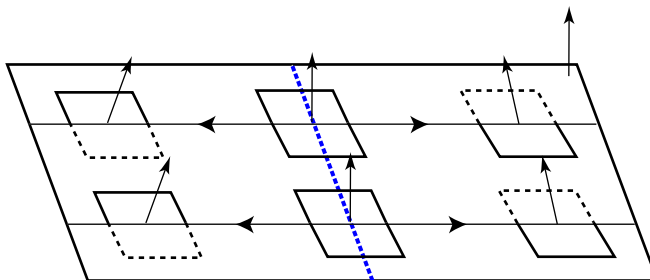


FIGURE 6. Legendrian divide.

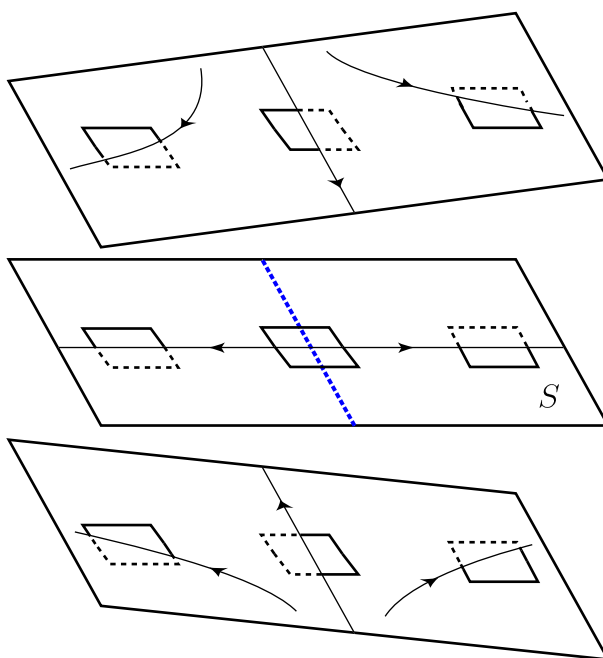


FIGURE 7. Flexibility near a Legendrian divide.

Example 4. *Proposition 3 gives sufficient, but not necessary conditions for a surface to be convex. Figure 6 shows a portion of convex surface whose induced foliation has a circle's worth of singularities. The circle of singularities is called a Legendrian divide. The contact structure hinted at in the figure is invariant under translation in the vertical direction or parallel to the Legendrian divide. Note that a Legendrian divide is not a dividing curve.*

Figure 7 shows a product neighborhood of the Legendrian divide and the effect of a slight perturbation of the original surface on the induced foliation.

This example hints at a remarkable theorem about the possible induced foliations that can occur on perturbations of a convex surface. Roughly, the

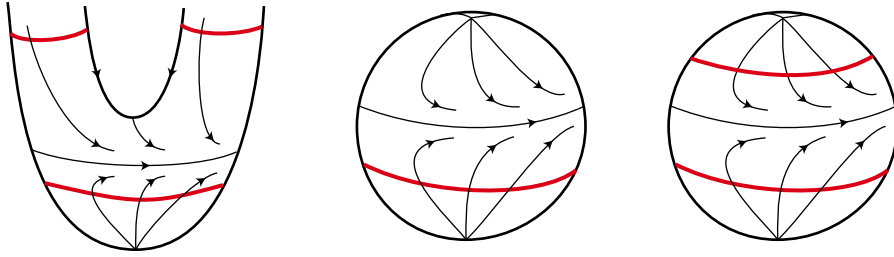


FIGURE 8. Hypothetical induced foliations.

Giroux Flexibility Theorem states that we can force the induced foliations to be whatever we like, within reason. The statement of the theorem will make more sense after reading the definitions which follow it.

Theorem 2 (Giroux Flexibility Theorem [18]). *Let $S \subset (M, \xi)$ be a convex surface with dividing set Γ_S , and let \mathcal{F} be an arbitrary singular foliation on S divided by Γ_S , then there exists an isotopy of S fixing Γ_S (and keeping S transverse to $\vec{\nu}$) such that at the end of the isotopy, \mathcal{F} is the induced foliation on S .*

Definition 5. Γ_S divides \mathcal{F} if Γ_S cuts S into a maximal number of sink and source regions, that is, regions in which the induced foliation either points in at every boundary component or out at every component of each region.

Example 5. Figure 8 shows three foliations. The first and last are divided by the indicated curves, but the middle example is not; it is not cut into a maximal number of sink and source regions as the third example shows. Another example to which the Giroux Flexibility Theorem can be applied is to replace the indicated foliation on the annular region between the two dividing curves of the third example with a Legendrian divide.

Definition 6. (M, ξ) is tight if there does not exist an embedded disk $D \subset M$ such that D is tangent to ξ along its boundary (i. e., $T_x D = \xi_x$ for all $x \in \partial D$). (M, ξ) is called overtwisted if it is not tight.

Overtwisted contact structures are classified by their underlying 2-plane bundles [11]. The notion of tightness is analogous to tautness or non-existence of Reeb components in foliation theory or incompressibility of surfaces. We shall see that tight contact structures reflect the underlying topology of the 3-manifolds which carry them.

Figure 9 shows an overtwisted disk that would live in the contact structure described in Example 1 if the contact planes were allowed to rotate too quickly along rays leaving the origin.

Proposition 4 (Giroux [19]). *If $S \subset (M, \xi)$ is convex, a product neighborhood of S is tight if and only if one of the following is satisfied:*

- (1) $S = S^2$, and Γ_S is connected

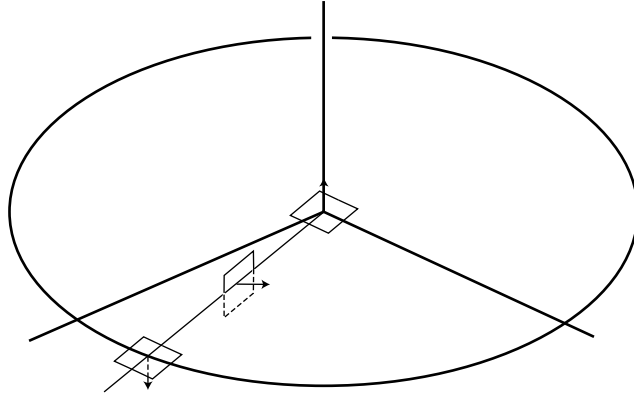


FIGURE 9. An overtwisted disk.

(2) $S \neq S^2$, and no component of Γ_S is null-homotopic in S .

Sketch. (\Rightarrow) If either (1) or (2) is false, use the Giroux Flexibility Theorem to realize a null-homotopic Legendrian divide, as discussed in Example 5. The disk in S bounded by the Legendrian divide will be an overtwisted disk.

(\Leftarrow) We need a starting point and gluing theorems. That is, until this point, we have not even stated that there are any tight contact structures on any manifold. The next theorem will address this. Given simple examples of tight contact structures we require gluing theorems to produce more complicated examples. This paper will eventually describe several gluing theorems. Another strategy, used by Giroux, is to produce models in which the desired S and Γ_S exist and must be tight. \square

Theorem 3. *There exist a tight contact structure on B^3 , moreover, two tight contact structures which induced the same foliations on B^3 are diffeomorphic.* \square

The existence portion of the theorem is due to Bennequin [1], and the uniqueness portion is due to Eliashberg [12]. In light of the Giroux Flexibility Theorem, we will paraphrase Theorem 3 by saying that there is a unique tight contact structure on B^3 .

Convex surfaces are required to have Legendrian boundary. Therefore to decompose manifolds with convex boundaries along convex surfaces, we will need to know which curves on a convex surface S can be “made Legendrian”. That is, we need to know which curves are contained in the leaves of some foliation \mathcal{F} divided by Γ_S . S can be perturbed so that they become Legendrian. The next definition and theorem of Honda’s [20] exactly answers this question.

Definition 7. *A properly embedded 1-submanifold C of a convex surface S is non-isolating if*

- (1) C is transverse to Γ_S and
- (2) the closure of every component of $S \setminus (\Gamma_S \cup C)$ intersects Γ_S .

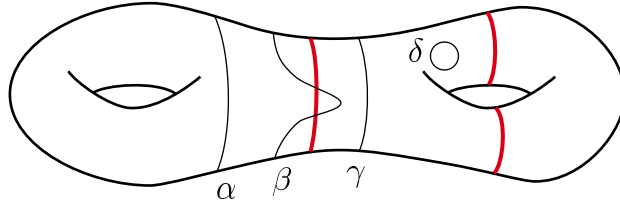


FIGURE 10. Hypothetical Legendrian curves.

Theorem 4 (Legendrian Realization Principle). *If C is non-isolating then C can be made Legendrian.*

Sketch. The non-isolating condition guarantees that C can be extended to a foliation divided by Γ_S . Then use Giroux Flexibility to realize this foliation on S . \square

Example 6. *Of the curves shown in Figure 10, only β and γ are non-isolating. Notice that any curve, such as β , which intersects Γ_S is non-isolating. It is not too hard to extend, say β , to a singular foliation on S divided by Γ_S , however β will end up passing through singularities, that is, it will not be a smooth curve on S . Note also that in the definition of non-isolating, C is not necessarily connected or closed.*

2. PREVIEW

At this point we have enough of the foundational tools in place to sketch, in general terms, some of the issues and techniques involved in studying contact structures from a cut-and-paste point of view.

Classification: Given a 3-manifold M and a collection of curves Γ contained in ∂M , how many tight contact structures, up to equivalence, are there on M with $\Gamma_{\partial M} = \Gamma$? Equivalence might be either diffeomorphism or isotopy taking one contact structure to another.

To be specific, consider the case of a solid torus with four dividing curves on its boundary shown in Figure 11.

Decomposition: How many “sensible” ways are there to decompose such an (M, Γ) ?

Continuing with the solid torus example, Figure 11 suggests that there are just two possible decompositions, thus, there are at most two tight contact structures carried by (M, Γ) .

Gluing: Which of the decompositions into tight pieces can be glued to form a tight union?

Unlike many situations in 3-dimensional topology, it is very difficult to give general conditions under which the union of tight pieces is tight. The problem is that a manifold can contain a large overtwisted disk, but when

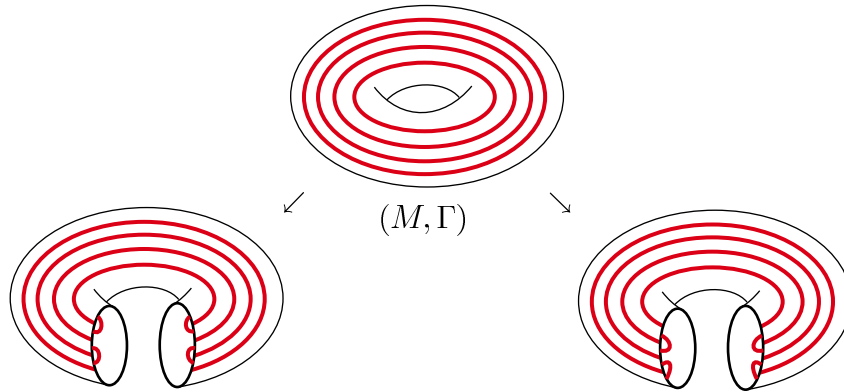


FIGURE 11. Different convex decompositions.

it is chopped into small pieces, none of the pieces may contain overtwisted disks themselves.

It turns out that regluing either of the decompositions shown in Figure 11 gives a tight contact structure. *A priori*, we do not know that these two contact structures are different. By gluing we can conclude only that (M, Γ) carries at least one tight contact structure.

Invariants: Of the various ways of gluing into a tight union, which result in non-isotopic contact structures?

In our example, an Euler characteristic type invariant shows that the two gluings result in different contact structures. It follows that (M, Γ) carries exactly two tight contact structures.

3. CONVEX DECOMPOSITIONS

A convex decomposition can be viewed in two ways. First, you can start with a contact structure on a 3-manifold M and keep splitting M along convex surfaces until the pieces are balls. Alternatively, you can start with M and a collection of curves Γ on ∂M that you hope will end up being dividing curves for a contact structure that you are trying to build, and then split along surfaces which you hope will end up being convex. We need to see how actual convex surfaces intersect so that this structure can be correctly modelled in the definition of a convex decomposition.

Example 7. The kernel of $\alpha_k = \sin(2\pi kz)dx + \cos(2\pi kz)dy$ defines a contact structure on \mathbb{R}^3 shown in Figure 12. In this example, the contact planes all contain the z -axis, that is, any vertical line is Legendrian. The foliation induced on horizontal planes is a linear foliation with slope changing as the height of the plane increases. The vector field given by $\frac{\partial}{\partial r}$ in cylindrical coordinates is a contact vector field, thus a cylinder at constant distance from the z -axis is convex. The dividing curves on this cylinder start on the x -axis

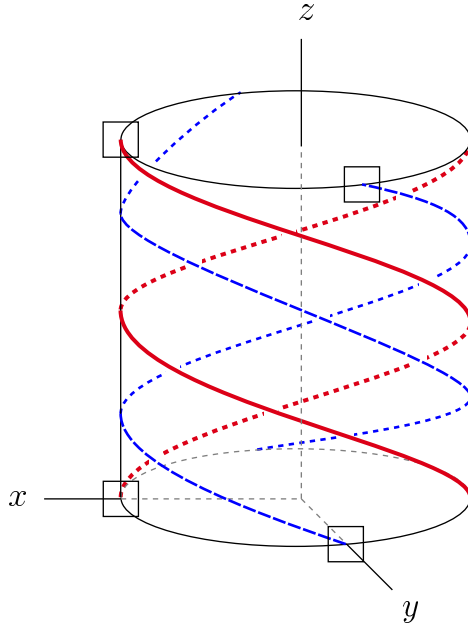


FIGURE 12. The neighborhood of a Legendrian curve.

and spiral upwards at a rate depending on k . Figure 12 also shows the tangencies of the contact planes and the cylinder as long dashed lines starting on the y -axis.

By restricting to the cylinder about the z -axis and identifying top and bottom, α_k also defines a contact structure on $S^1 \times D^2$. The key features of this contact structure are:

- (1) $T = \partial(S^1 \times D^2)$ is convex
- (2) $\#\Gamma_T = 2$
- (3) $\text{slope}(\Gamma_T) = -\frac{1}{k}$

The next theorem may be paraphrased by saying that Legendrian curves, such as the quotient of the z -axis in the previous example, have standard neighborhoods.

Theorem 5 (Kanda [25], Makar-Limanov [26]). *There is a unique tight contact structure on $S^1 \times D^2$ such that (1), (2), and (3) hold.* \square

When we start with a manifold with convex boundary and cut it along a convex surface, the cutting surface, by definition of convexity, intersects the boundary in a Legendrian curve. The next example is a portion of the region shown in Figure 12. From it we see how the dividing curves on a pair of intersecting surfaces are related near their Legendrian curve of intersection.

Example 8. *In Example 7 the xz -plane is convex with respect to the contact vector field $\frac{\partial}{\partial y}$ and similarly the yz -plane is convex with respect to $\frac{\partial}{\partial x}$.*

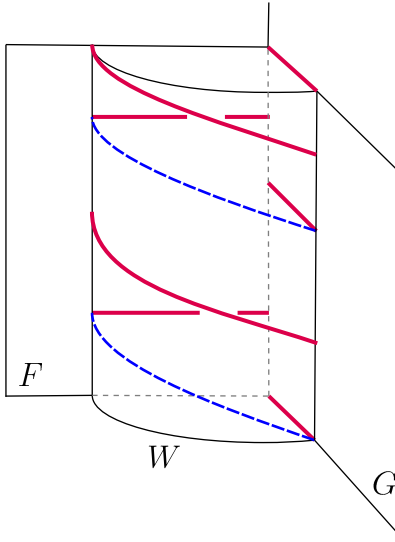


FIGURE 13. Intersecting convex surfaces.

Figure 13 shows portions of these planes, labelled F and G and their dividing curves. Notice that Γ_F and Γ_G are horizontal lines starting on the z -axis and ending at a point of tangency of a contact plane and the vertical cylinder.

From this we see that for general intersecting convex surfaces F and G , the endpoints of Γ_F and Γ_G alternate along curves of $F \cap G$. Further examination of Figure 13 shows that if the corner of the wedge W subtended by F and G is smoothed, the manifold produced has convex boundary and the dividing curves of F and G are joined by turning to the right (when viewed from the outside of W). The “turn to the right” rule that is forced on us in the presence of a *positive* contact structure serves as the model for defining the orientation conventions in convex decompositions.

Figure 14 shows three views of W . The first shows W before rounding corners, the second is after rounding corners. The last picture shows W without the corner rounded, but it shows the effect on the dividing curves of corner rounding. Most of the figures in this paper are drawn in this fashion.

Definition 8. (M, γ) is a sutured manifold if:

- (1) $\gamma \subset \partial M$ is a union annuli and tori,
- (2) $(\partial M) \setminus \gamma$ is a disjoint union of two subsurfaces $R_+(\gamma)$ and $R_-(\gamma)$,
and
- (3) crossing an annular suture takes you from $R_\pm(\gamma)$ to $R_\mp(\gamma)$.

Gabai [14] defined sutured manifolds to study taut foliations. We will primarily be concerned with that case that all sutures are annuli. Figure 15 shows two views of a solid ball with a single annular suture. The first view shows a manifold with corners, as it should be drawn. The second shows

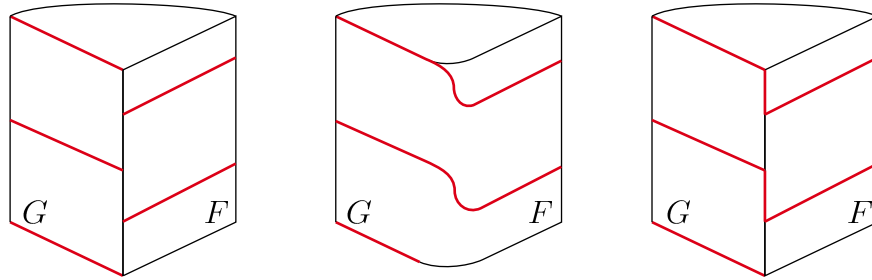


FIGURE 14. Dividing curves before and after smoothing.

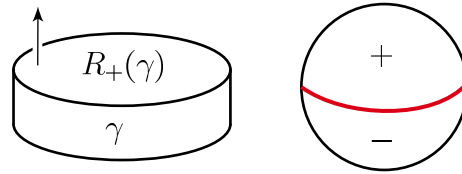
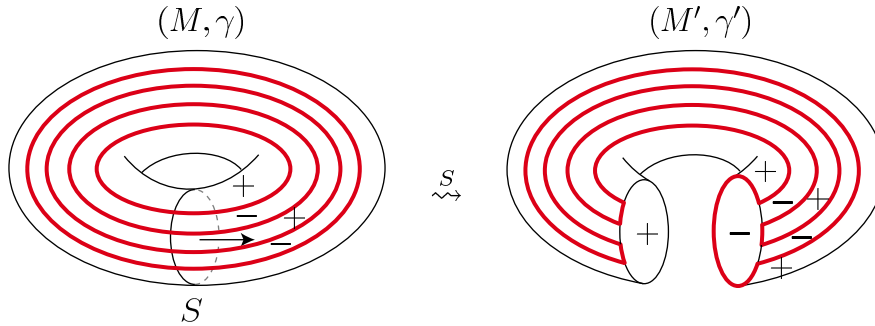
FIGURE 15. B^3 with a single suture.

FIGURE 16. Sutured manifold splitting.

how sutures will be drawn; the manifold appears smooth, and the sutures are very skinny.

Definition 9. If S is an oriented properly embedded surface in (M, γ) , $(M, \gamma) \xrightarrow{S} (M', \gamma')$ is defined by $M' = M \setminus S$ and introducing sutures as needed to separate the positively and negatively oriented portions of $\partial(M \setminus S)$ as shown in Figure 16.

Definition 10. A convex structure is a pair (M, Γ) such that:

- (1) Γ is a disjoint union of curves in ∂M ,
- (2) ∂M split along Γ is the disjoint union of two subsurfaces, $R_+(\Gamma)$ and $R_-(\Gamma)$, and
- (3) crossing a dividing curve takes you from $R_\pm(\Gamma)$ to $R_\mp(\Gamma)$.

Also assume each component of ∂M has dividing curves on it.

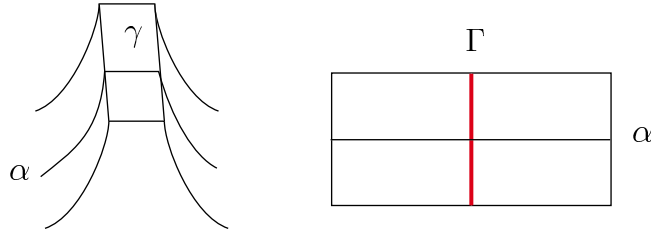


FIGURE 17. An arc crossing a suture compared to an arc crossing a dividing curve.

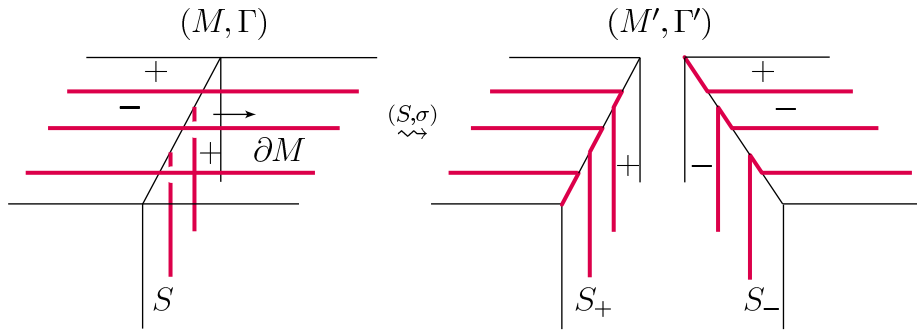


FIGURE 18. A convex splitting,

A sutured manifold (M, γ) is a manifold with corners. Convex structures (M, γ) are smooth. Figure 17 shows portions of a sutured manifold near a suture and a convex structure near a dividing curve. Notice that the 2-planes along each arc α turn over as α is traversed, but they do so in different fashions.

Of course we hope that (M, Γ) will carry an actual tight contact structure, just as Gabai would like (M, γ) to carry a taut foliation; however there is no *a priori* reason that it will. When discussing a surface with curves on it, such as (S, σ) in the next definition, there is no need to distinguish between an “abstract” convex surface and an actual convex surface, for a contact structure is uniquely determined in a (product) neighborhood of S by the dividing curve configuration σ .

Definition 11. Let (S, σ) be a convex surface in (M, Γ) such that ∂S is non-isolating in ∂M , and the endpoints of σ alternate with points of $\Gamma \cap \partial S$ along ∂S . Define $(M, \Gamma) \xrightarrow{(S, \gamma)} (M', \Gamma')$ by $M' = M \setminus S$ and by adding new portions of dividing curves to $(\sigma \cup \Gamma) \setminus S$ using the “turn to the right” rule shown in Figure 18.

A sutured manifold with annular sutures (M, γ) naturally determines a convex structure (M, Γ) by replacing each annulus of γ by its core. To be able to use Gabai’s existence theorems for sutured manifold decompositions in our setting we must be able to start with a sutured manifold splitting

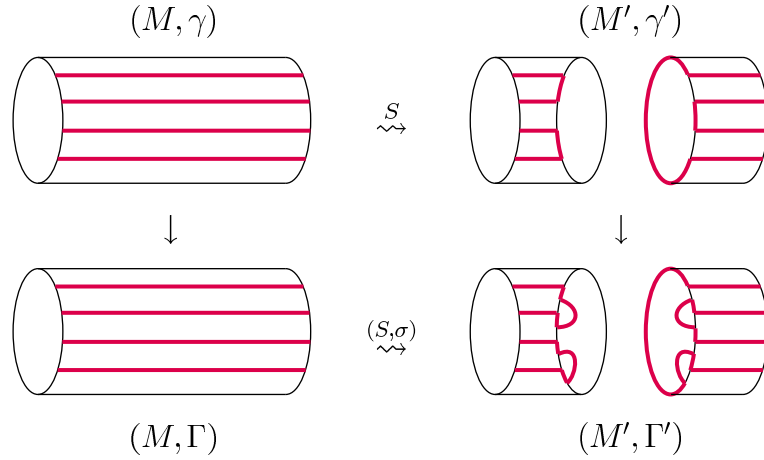


FIGURE 19. A commuting diagram of sutured manifold and convex splittings.

(the top row of the following diagram) and then produce a convex surface, (S, σ) , such that the diagram commutes. We discuss how this can be done through a series of examples.

$$\begin{array}{ccc}
 (M, \gamma) & \xrightarrow{\sim S} & (M', \gamma') \\
 \downarrow & & \downarrow \\
 (M, \Gamma) & \xrightarrow{\sim (S, \sigma)} & (M', \Gamma')
 \end{array}$$

Example 9. Figure 19 shows how to introduce boundary-parallel dividing curves, σ , so that the diagram commutes. This technique works, provided that every component of ∂S has nonempty intersection with Γ .

Definition 12. A convex surface (S, σ) has boundary-parallel dividing curves if ∂S is nonempty, every component of ∂S intersects σ , and σ is collection of arcs each of which bounds a half disk that contains a portion of ∂S but no other arcs of σ .

Example 10. Now consider the possibility that $\partial S \cap \Gamma = \emptyset$. Such an S might have isolating boundary, that is, it might not be possible to make it Legendrian and hence S convex. Figure 20 shows first a sutured manifold splitting along a surface S with $\partial S \cap \Gamma = \emptyset$. The second two portions of the figure show two possible ways of introducing intersections between ∂S and Γ and of adding boundary compressible σ to S .

There are two key features in this example. First, the strategy of introducing intersections can only work if there are dividing curves on the same component of ∂M as ∂S – this will show up in the definition of “sutured manifold with annular sutures” below. And second, only one of the perturbations of S makes the splitting diagram commute.

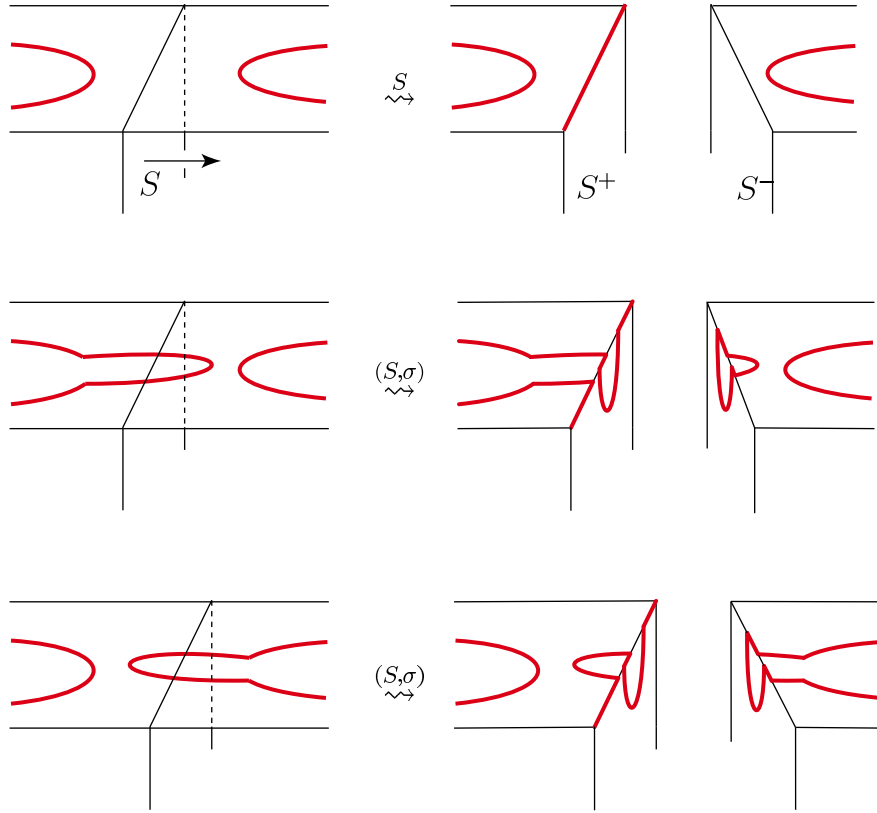


FIGURE 20. Two possibilities for (S, σ) .

Figure 21 is similar to Figure 20 in that $\partial S \cap \Gamma = \emptyset$, but in this case there are multiple portions of ∂S , each with its own orientation preference for creating a pair of intersections with Γ , and they can not all be satisfied simultaneously. Rather than describe how to get around this, we just point out that Gabai confronted a similar situation in developing sutured manifold theory. He introduced a notion of “well-groomed” sutured decompositions, that is, he showed that splittings could be assumed to have coherently oriented boundary components, and for such splittings we can produce a commutative splitting diagram using the technique of Example 10.

Theorem 6. *Let (M, γ) be an irreducible sutured manifold with annular sutures, and let (M, Γ) be the corresponding convex structure. The following are equivalent.*

- (1) (M, γ) is taut.
- (2) (M, γ) has a sutured manifold decomposition.
- (3) (M, γ) carries a taut foliation.
- (4) (M, γ) carries a universally tight contact structure.
- (5) (M, γ) carries a tight contact structure.

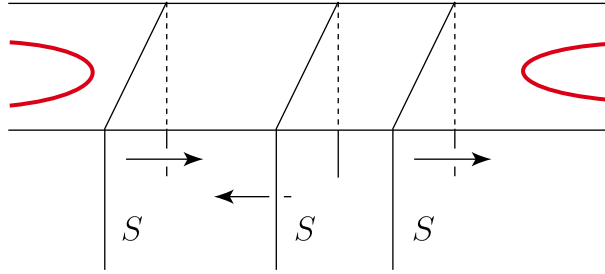


FIGURE 21. There is no consistent way to introduce intersections between ∂S and Γ .

Definition 13. A sutured manifold has annular sutures if ∂M is nonempty, every boundary component contains at least one annular suture, and if there are no toroidal sutures.

(M, γ) is taut if $R_+(\gamma)$ and $R_-(\gamma)$ are Thurston norm minimizing in their homology class in $H_2(M, \gamma)$.

A sutured manifold decomposition of M is a sequence of splittings

$$(M, \gamma) \xrightarrow{S_1} \dots \xrightarrow{S_m} \cup (B^3, S^1 \times I)$$

where $(B^3, S^1 \times I)$ denotes the sutured manifold shown in Figure 15.

A foliation is taut if every leaf intersects a closed transversal.

A contact structure is universally tight if $(\widetilde{M}, \widetilde{\xi})$ is tight.

Thurston [28] proved (3) implies (1). Gabai [14] proved (1) implies (2) and (2) implies (3). Eliashberg and Thurston [13] showed (3) implies (4). It is immediate that (4) implies (5). All of these results apply without the additional assumption of annular sutures. Since S^3 carries a tight contact structure but can not support a taut foliation, some additional hypothesis is necessary for (5) to imply (1).

The techniques of (5) implies (1) will not be used in the rest of the paper, so we will instead sketch a direct proof of (2) implies (4) that has the advantages of making the importance and utility of universal tightness clear. The proof introduces a gluing strategy that will be used repeatedly.

Proof of (2) implies (4). First replace the given sutured manifold decomposition with a corresponding convex decomposition

$$(M, \Gamma) \xrightarrow{(S_1, \sigma_1)} \dots \xrightarrow{(S_m, \sigma_m)} \cup (B^3, S^1)$$

By Theorem 3, (B^3, S^1) carries a (universally) tight contact structure. By construction, the surfaces (S_i, σ_i) have boundary-parallel dividing curves (see Definition 12) thus this portion of the theorem follows from the next gluing theorem. \square

Theorem 7. (Colin [7]) Let $(M, \Gamma) \xrightarrow{(S, \sigma)} (M', \Gamma')$. If M is irreducible, S has boundary compressible dividing curves, and (M', Γ') carries a universally tight contact structure then so does (M, Γ) .

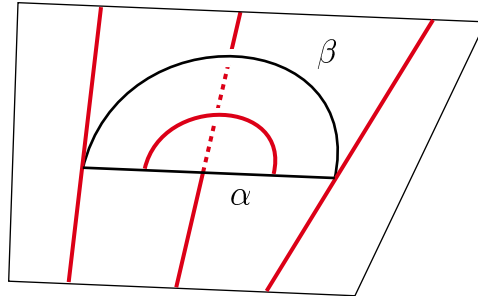


FIGURE 22. A bypass attached to S along α .

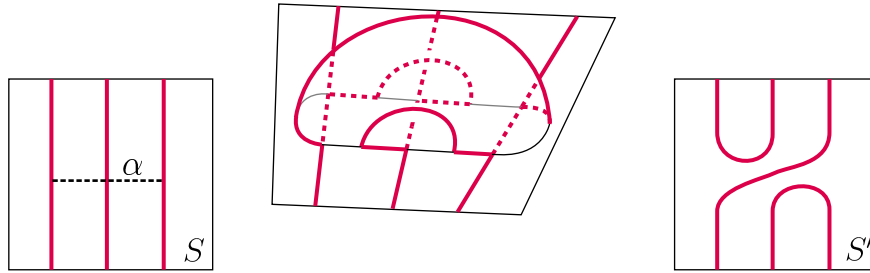


FIGURE 23. The effect on Γ_S of isotoping S through a bypass attached along α .

Sketch. We will illustrate key ideas of our interpretation [22] of Colin’s gluing theorem with examples. The proof strategy is to:

- (1) Suppose the contact structure on (M, Γ) obtained by gluing (M', Γ') along (S, σ) is overtwisted, and let D be an overtwisted disk.
- (2) In *small steps* isotop S to S' and eventually off D .
- (3) While isotoping S , make sure that $M \setminus S'$ stays universally tight.

This strategy gives a contradiction once $S' \cap D = \emptyset$, for $M \setminus S'$ is both tight and contains the overtwisted disk D .

In *small steps* refers to a fundamental idea due to Honda [21]. That is, any isotopy of a convex surface S can be expressed as a sequence of *bypasses* or their inverses.

Definition 14. A bypass consists of:

- (1) a Legendrian arc α connecting 3 dividing curves in S .
- (2) a Legendrian arc β joining $\partial\alpha$
- (3) a convex half disk in $M \setminus S$ with boundary equal to $\alpha \cup \beta$ which contains a single dividing curve.

Figure 23 shows the effect on σ of isotoping S across a bypass. Notice that the “turn to the right” rule for dividing curves going around corners looks more like a “turn to the left” rule when it is viewed from inside the manifold.

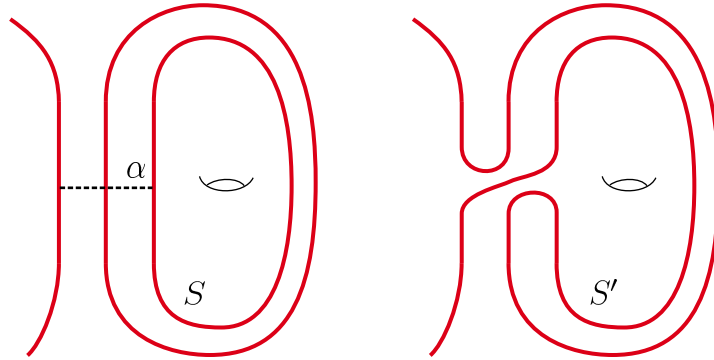


FIGURE 24. This bypass removes two parallel dividing curves.

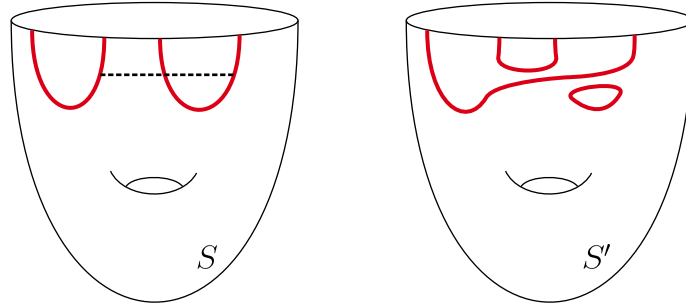


FIGURE 25. This bypass can not exist in a tight contact structure.

Example 11. *The global effect on the dividing curves of a bypass move depends very much on how the local picture sits with respect to the entire surface and dividing curve set. Figure 24 shows an example in which the arc of attachment connects two parallel dividing curves to a third. Isotoping S across this bypass has the effect of removing two dividing curves from S .*

Continuing with the gluing theorem, we now consider some examples of bypasses that S might have to be isotoped through while moving S off of D . Hopefully universal tightness of $M \setminus S'$ follows from universal tightness of $M \setminus S$ in each case.

Example 12. *Notice that the dividing curves in Figure 25 are boundary-parallel. If such a bypass were to exist in M , then, as shown, S' would contain a null-homotopic dividing curve. Proposition 4 implies the existence of an overtwisted disk near S' . Since S' may be thought of as living in the complement of S , and we are assuming $M \setminus S$ is universally tight, the bypass drawn in Figure 25 can not exist.*

Example 13. *Figure 26 shows a similar-looking bypass that has a very different effect on the dividing curves of σ . Up to isotopy, the dividing curves are unchanged. Though we omit the proof here (see [22]), it is a consequence*

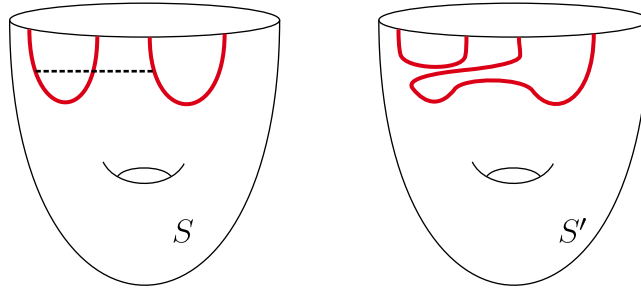


FIGURE 26. A trivial bypass.

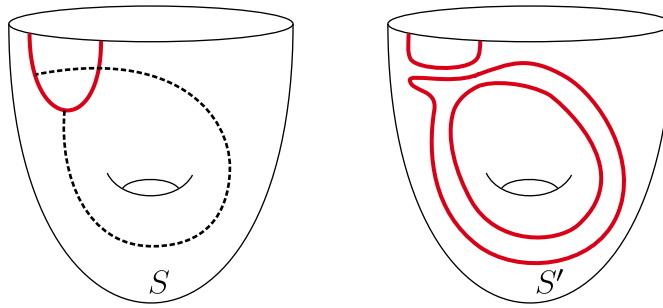


FIGURE 27. It isn't clear what the implications of such a bypass are in general.

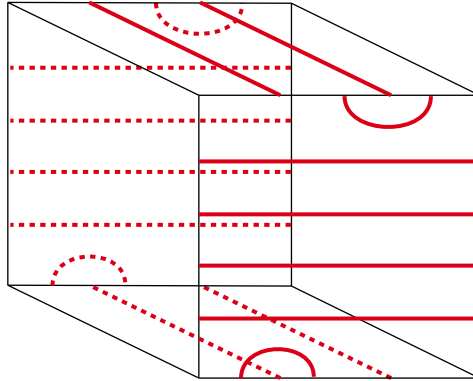
of the uniqueness of tight contact structures on a ball that S and S' cobound a contact product. It follows that $M \setminus S$ and $M \setminus S'$ are contactomorphic, hence both are universally tight.

Example 14. Figure 27 is the most mysterious of these examples. Such a bypass may or may not exist, and there is no reason for $M \setminus S'$ to be tight if we only assume tightness of $M \setminus S$. However, α represents a nontrivial element of $\pi_1(S)$ or $\pi_1(M)$, and any cover $\widehat{M} \setminus S$ is still tight (by universal tightness). If we lift to the right cover, α is unwound, and this example becomes the same as the previous example. Thus the proof strategy may be continued in this and subsequent covers.

There are several other types of bypass configurations to check, but this pattern repeats itself. Bypasses are of three types. Those which can not exist. Those which cause no trouble if they do exist, and all of the rest. The typical situation is that troublesome bypasses can be dealt with in the right cover. This is the point and power of the assumption of universal tightness. \square

4. TORI

Example 15. Let $\alpha_k = \sin(2k\pi z)dx + \cos(2k\pi z)dy$ as in Example 7. Restricting α_k to the cube $[0, 1] \times [0, 1] \times [0, 1]$ and identifying the front with the

FIGURE 28. ξ_2 on $T \times I$.

back face and the left with the right face defines a contact structure on $T \times I$. Neither $T \times \{0\}$ nor $T \times \{1\}$ is convex. Perturbing $T \times \{0\}$ and $T \times \{1\}$ so that they are convex gives the contact structure ξ_k on $T \times I$ shown in Figure 28. A vertical annulus, such as the one shown on the front face, will be convex and have $2k$ closed dividing curves.

The next theorem gives a very general, but rough, classification theorem for tight contact structures.

Theorem 8. *If M is irreducible, then M carries finitely many tight (or universally tight) contact structures if and only if M is atoroidal.*

The if direction is due to Colin, Honda, and Giroux [10], and the only if direction is due to Colin [8, 9] and Honda, Kazez, and Matić [22].

Proof. We will explain the following portions of the proof of finiteness direction:

- (1) There is a finite collection of branched surfaces in M which carry every tight contact structure.
- (2) If a branched surface carries infinitely many tight contact structures then it carries tori.

Proof of (1).

- Pick a triangulation τ of M , and isotop it until τ^1 is a collection of Legendrian arcs.
- Isotop τ^2 relative to τ^1 so that each face is convex.
- Isotop τ to remove interior ∂ -parallel dividing curves. Figure 29 shows how to pry a two cell open along an edge to effect a bypass move and accomplish this.
- For each $\Delta \in \tau^3$, group the dividing curves in $\partial\Delta^3$ so that, except for a bounded number of dividing curves near the vertices, they are contained in at most 5 prisms P_i . See Figure 30.

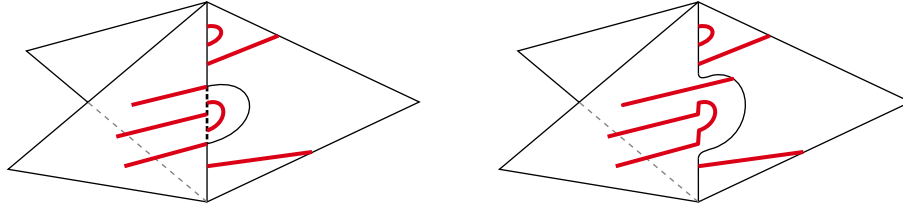


FIGURE 29. Isotoping an edge of τ across a bypass.

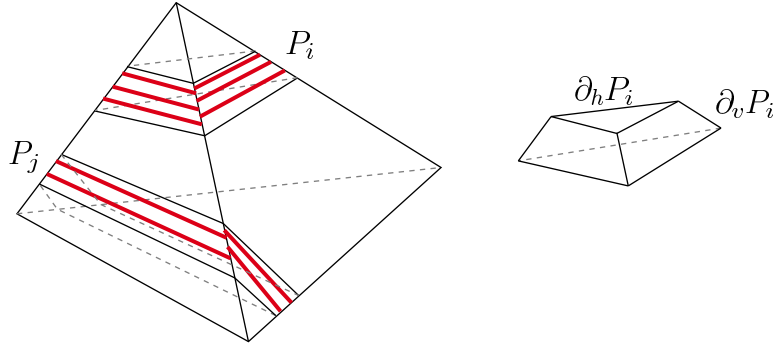


FIGURE 30. Dividing curves on $\partial\Delta$ are carried by a family of prisms.

- Use Giroux Flexibility to force the foliation induced by ξ on each $\partial_v P_i$ to be a union of vertical arcs and on $\partial_h P_i$ to be a fixed non-singular foliation.
- By the uniqueness of tight contact structures on B^3 we may assume all vertical arcs in P_i are Legendrian.
- The union over $\Delta \in \tau^3$ is naturally a neighborhood $N(B)$ of a branched surface B , and by construction there are only finitely many such B .
- Each component of $\Delta^3 - N(B)$ is a polygonal ball. The number of such polygonal balls is bounded, and the possible dividing curve configurations on the boundary faces of each polygonal ball is also bounded. Thus ξ is defined by $\xi \upharpoonright N(B)$ up to finitely many choices.

Proof of (2).

Suppose two contact structures ξ_0, ξ_1 are carried by B . By construction the foliations induced on $\partial_h N(B)$ agree, thus ξ_1 is defined by ξ_0 and a finite set of integer weights on the sectors of B which describe the twisting of the planes of ξ_1 relative to the planes of ξ_0 along vertical Legendrian arcs of $N(B)$.

An infinite collection of contact structures all carried by one branched surface give an infinite collection of weights. Since the contact structures are all positive, there is a lower bound, perhaps negative, on these weights. It follows that there must be a non-negative collection of integer weights on

B . In the standard way, these non-negative weights can be used to piece together a surface in $N(B)$ that is transverse to the vertical Legendrian arcs. The induced foliation on such a surface has no singularities, thus the surface is either a torus or a Klein bottle.

We draw two conclusions from this portion of the argument.

- Changing weights along a torus doesn't change the homotopy class of the 2-plane bundle, thus it follows that only finitely many 2-plane bundles support tight contact structures.
- The only way to produce infinitely many contact structures on a given space is to insert ξ_k , as defined in Example 15, in a neighborhood of a torus.

With this in mind we sketch some of the remaining steps in the infinitely many portion of the theorem.

- (3) A toroidal manifold has a universally tight contact structure.
- (4) Inserting ξ_k near the torus preserves universal tightness
- (5) and changes the contact structure.

Proof of (3).

We will assume $\partial M = T$. This is just one gluing theorem away from full generality. The sutured manifold (M, T) , where T is a toroidal suture, is automatically taut, and by Gabai's theorem it has a sutured manifold decomposition. For simplicity, assume the first splitting surface S intersects T in a single curve, and say $(M, T) \xrightarrow{S} (M', \gamma')$.

We would like to consider the corresponding convex decomposition, but first we must fix the toroidal suture. Pick two parallel curves on T dual to $S \cap T$ and define them to be Γ . Figure 31 shows how we can force the usual correspondence between the sutured manifold decomposition on the first row and the convex structure on the second row. It is particularly important to note that (S, σ) has boundary-parallel dividing curves. Since (M', γ') has a sutured manifold decomposition, (M', Γ) carries a universally tight contact structure. By Theorem 7 (M, Γ) does also.

The technique of adding a pair of parallel dividing curves to a boundary component with no sutures can be used in other settings as well.

Proof of (4).

Continuing with the same M, S , and T , we need to show that the contact structure on $M \cup (T \times I)$ obtained by gluing the structure built in (3) and ξ_k is universally tight. Gluing along T is beyond the scope of Theorem 7. Instead we will compare

$$(M, \Gamma) \xrightarrow{(S, \sigma)} (M \setminus S, \Gamma')$$

and

$$M \cup \xi_k \xrightarrow{S \cup A} (M \setminus S) \cup (T \times I \setminus A)$$

where S is the first decomposing surface, and A is an annulus extending ∂S that is used to keep track of the k twists in ξ_k .

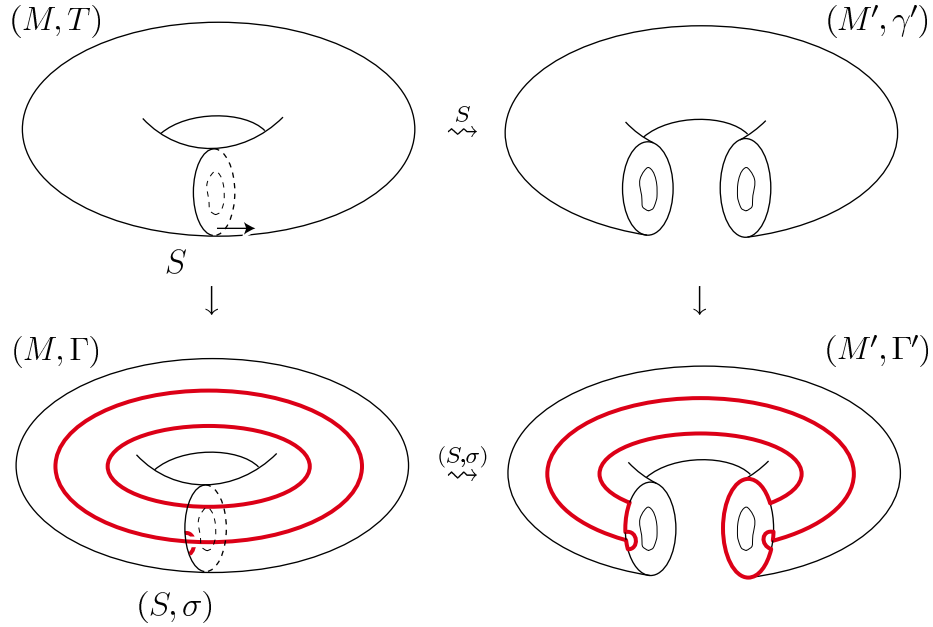


FIGURE 31. Introducing dividing curves on a torus suture.

The first row of Figure 32 shows two views of $M \setminus S$ near $T \setminus S$. In the first 3-dimensional picture, a pair of dividing curves becomes a single dividing curve after corner rounding. In the second, the same neighborhood is expressed as a product with S^1 , and the single dividing curve is shown as a point. The second row of the figure gives a similar view of $(M \setminus S) \cup (T \times I \setminus A)$ in the case $k = 1$. The product with S^1 view also shows a convex surface transverse to the S^1 direction that detects the twisting along ξ_k .

We now show that our contact structure $(M \setminus S) \cup (T \times I \setminus A)$ is tight. This will be done by finding an embedded copy of this space in the tight space $M \setminus S$, and then using the obvious (but useful!) fact that a subset of a tight space is tight. Here is how this is done.

The curve C parallel to ∂S shown in Figure 33 is isolating. Pass to a cover, without changing notation, in which the number of boundary components of S is increased, and then C becomes non-isolating. Then use flexibility to make C a Legendrian divide. Figure 34 shows a product with S^1 view of $M \setminus S$ near $T \setminus S$. The region shown is the product of a convex disk and S^1 . This disk is shown with part of two dividing curves that end on the two points of intersection with C , and these two points of C are shown as hollow dots.

Figure 35 shows $(M \setminus S) \cup (T \times I \setminus A)$. Finally, Figure 36 shows a larger version of $(M \setminus S)$ than Figure 34. The shaded subset of Figure 36 is contact isomorphic to $(M \setminus S) \cup (T \times I \setminus A)$ and is necessarily (universally) tight.

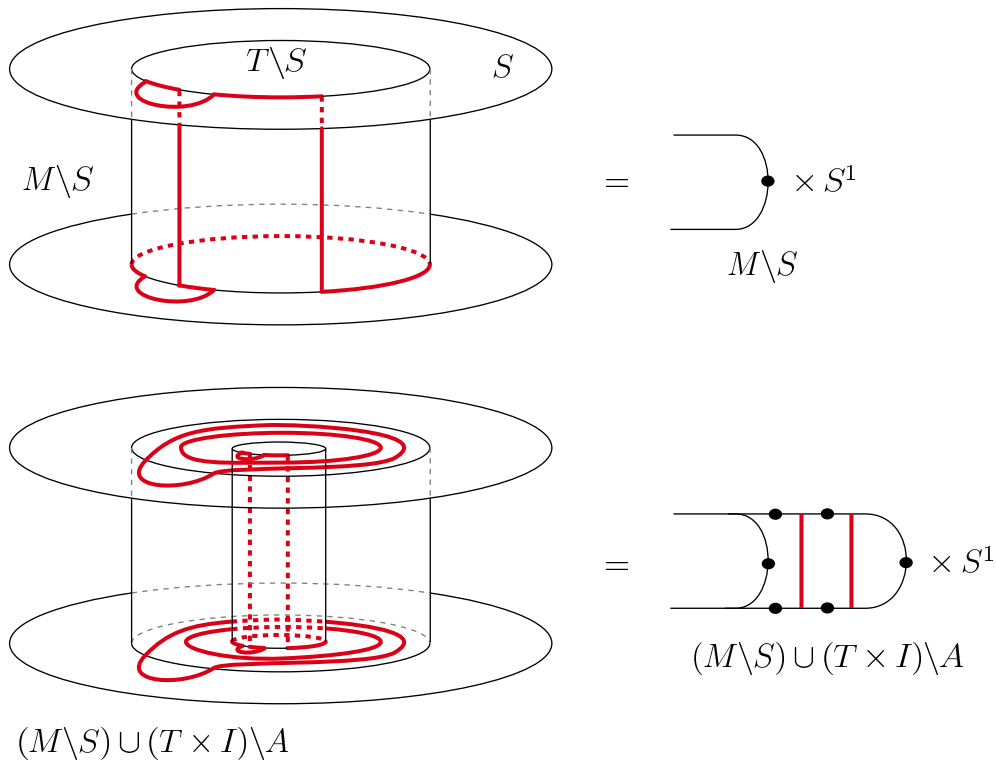


FIGURE 32. Views of $M \setminus S$ near the boundary before and after adding $T \times I \setminus A$.

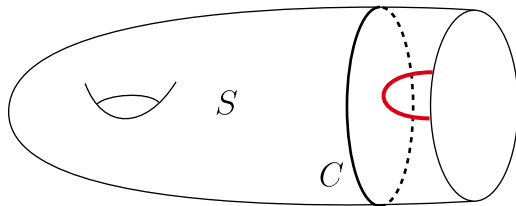


FIGURE 33. The curve C is isolating.

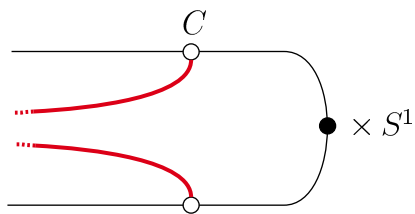


FIGURE 34. C is now a Legendrian divide.

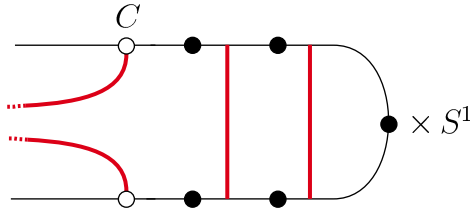


FIGURE 35. $M \cup (T \times I)$ split along $S \cup A$.

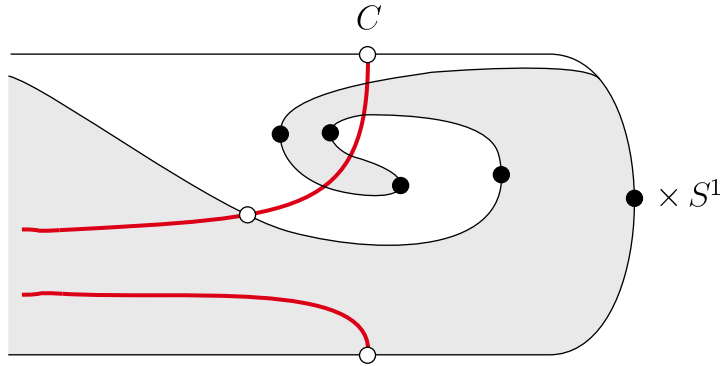


FIGURE 36. Enlarged view of $M \cup T$ split along S shown with a distinguished subset.

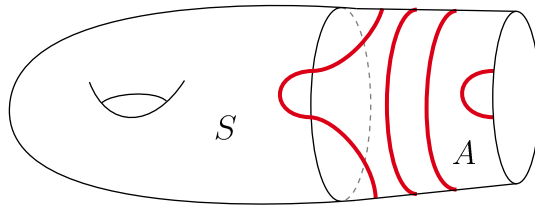


FIGURE 37. Dividing curves on $S \cup A$.

Next we show the contact structure on $M \cup (T \times I)$ is tight. This will require a gluing theorem along $S \cup A$, which unlike S , does not have boundary-parallel dividing curves. Figure 37 shows $\Gamma_{S \cup A}$.

We will use the same gluing strategy:

- (a) Assume the union along $S \cup A$ is overtwisted.
- (b) Isotop, via bypasses, $S \cup A$ off of the overtwisted disk, and
- (c) argue that the split manifold stays tight during (b).

There is an important change in perspective though. From the point of view of $S \cup A$, performing an isotopy in (b) is equivalent to digging a bypass out of one side of $S \cup A$ and adding it to the other side. We prove (c) by showing that there are no troublesome bypasses that can be dug from either side of $S \cup A$ in $M \cup (T \times I)$.

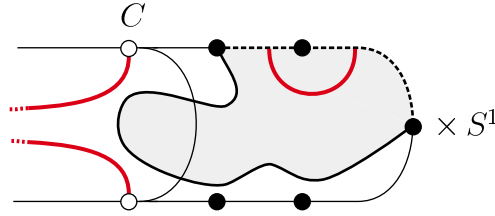


FIGURE 38. A possible location of a bypass.

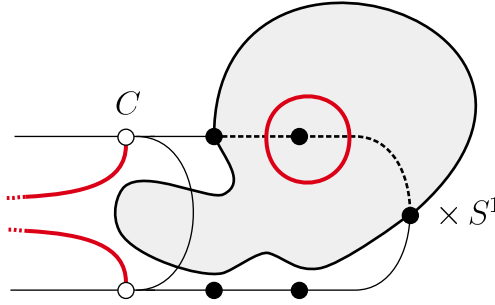


FIGURE 39. Detecting a bypass by adding a “template”.

We have discussed bypasses which involve only boundary compressible dividing curves in the proof of Theorem 7, so now we consider the existence of a bypass involving the closed dividing curves on $S \cup A$.

Example 16. *Figure 38 shows a bypass attached along a dotted curve α connecting three different dividing curves on the boundary of $(M \cup T \times I) \setminus (S \cup A)$. Figure 35 showed the same space, but it showed a convex disk with a different set of dividing curves. Certainly this bypass, if it exists, is not a subset of that convex disk. Indeed the bypass itself may be very large and reach out of the portion of the manifold shown in either of these figures.*

Proposition 5. *The bypass shown in Figure 38 can not exist.*

Proof. Consider the space obtained by adding the product of a bypass attached along α and S^1 that is shown in Figure 39. The null-homotopic dividing curve that is created implies the contact structure is overtwisted.

The opposite conclusion is reached if we add the same set and consider its relationship to the convex disk that we know is contained in $(M \cup T \times I) \setminus (S \cup A)$. The union is shown in Figure 40. We see that this space must be tight, for it too is a “fold along C ”, that is, it too can be found as a subset of $M \setminus S$. This completes the proof of the Proposition and hence Step (4). \square

Proof of (5).

We will only give the idea behind the technique used in producing invariants that distinguish the various contact structures on $M \cup (T \times I)$. Let

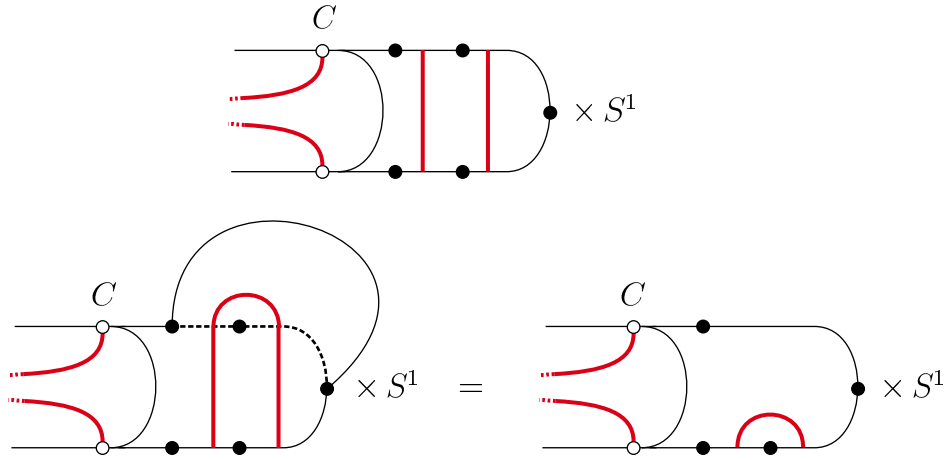


FIGURE 40. The actual result of adding the template.

F be a properly embedded convex surface which intersects the boundary component $T \times \{1\}$ of $M \cup (T \times I)$, and let δ be a homotopically essential arc in F which starts and ends on $T \times \{1\}$. The minimum of $\#\delta \cap \Gamma_F$ over all such δ and F is an invariant which tends to infinity as the twisting, that is, the k in ξ_k , is increased.

□

5. SURFACE BUNDLES

We will give a classification of tight contact structures on $\Sigma \times I$ such that

- (*) Σ is a closed surface with genus at least two, and the dividing curves on each component of $\partial(\Sigma \times I)$ are a pair of parallel non-separating curves.

Example 17. *In Figure 41, notice that on Σ_1 , $\chi(R_+) = \chi(\Sigma_1)$ and $\chi(R_-) = 0$. This is analogous to the product foliation on $\Sigma \times I$ in the sense that the contact 2-planes have outward pointing normal vectors everywhere on Σ_1 , at least as measured by Euler characteristic. This structure is a special case of an extremal contact structure.*

Definition 15. *A contact structure on a surface bundle with fibre Σ is extremal if the Euler class of the 2-plane bundle, $e(\xi)$, satisfies $e(\xi)(\Sigma) = \pm\chi(\Sigma)$. Equivalently, if Σ is convex either $\chi(R_+) = \chi(\Sigma)$ or $\chi(R_-) = \chi(\Sigma)$.*

Theorem 9. [23] *There are exactly 4 (universally) tight non-product contact structures satisfying (*). They correspond to a choice of dividing curve on each of Σ_0 and Σ_1 .*

This theorem will be used to prove the following theorems.

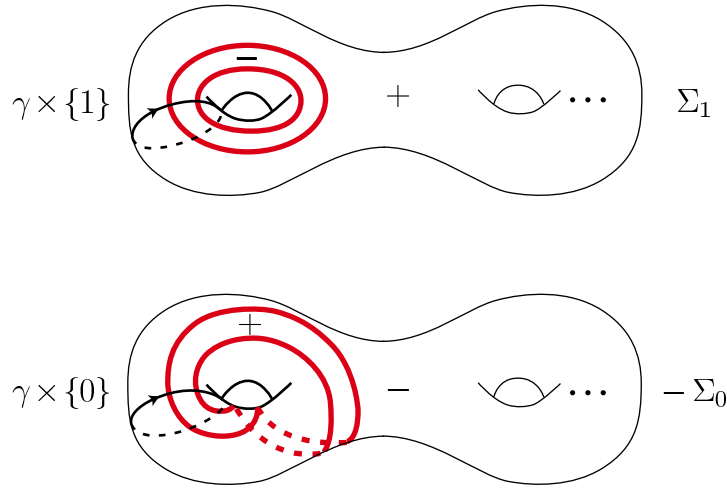


FIGURE 41. Dividing curves and splitting annulus on $\Sigma \times I$.

Theorem 10. *Let φ be a pseudo-Anosov map of a closed surface Σ . There is a unique extremal, tight (or universally tight) contact structure on $(\Sigma \times I)/(\varphi(x), 1) \sim (x, 0)$.*

Theorem 11. *(Gabai-Eliashberg-Thurston Theorem) If M is Haken and $H_2(M) \neq 0$, then M carries a universally tight contact structure.*

Theorem 11 follows from Gabai's work [14] on the existence of taut foliations and Eliashberg and Thurston's perturbation technique [13] for producing universally tight contact structures from taut foliations. The proof we give [24] is a direct construction which has the advantage of helping us discover new gluing theorems.

Sketch of Theorem 9. We concentrate only on the dividing curve configuration shown in Figure 41. What the proof strategy lacks in subtlety it makes up in directness. We start by decomposing $\Sigma \times I$ along a vertical annulus $\gamma \times I$ whose boundary components are shown in Figure 42 and analyze all possible dividing curve configurations.

Figure 43 shows $\gamma \times I$ cut by a vertical arc into a rectangle, and it lists all possible dividing curve configurations such that the boundary components of $\gamma \times I$ intersect the dividing curves twice each.

We will show how Type II_2^+ can be reduced to Type II_0^+ , that is, if we start with a convex annulus of Type II_2^+ , we can find another convex annulus of Type II_0^+ . This case is fairly typical of the type of arguments we use to prove this classification theorem.

Figure 43(A) shows the result of splitting $\Sigma \times I$ along an annulus of Type II_2^+ , and Figure 43(B) shows the dividing curves on $\Sigma \setminus \sigma \times \{0\}$. After rounding the corners and gathering the dividing curves on the two vertical annuli of $(M \setminus \sigma) \times I$, the result is shown in Figure 43(C). Cut this along

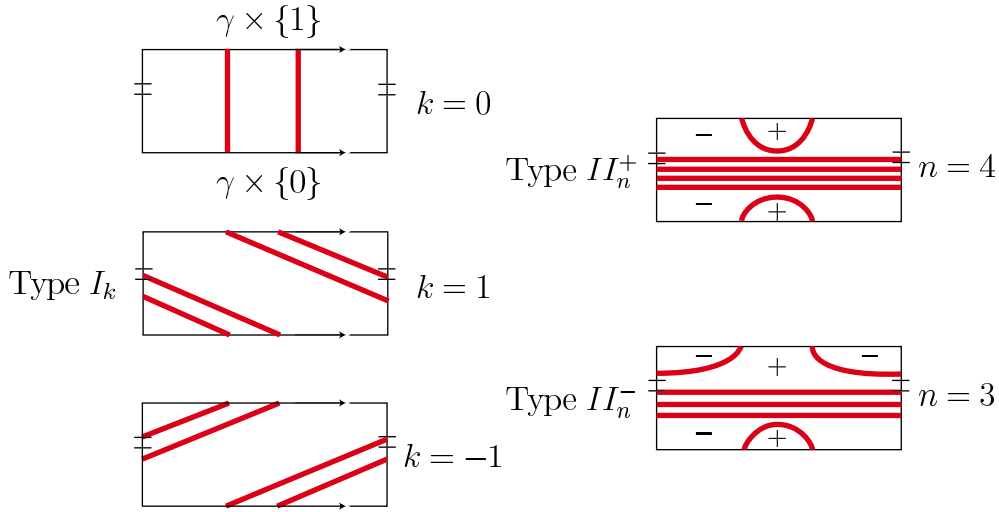


FIGURE 42. Possible dividing curves on $\gamma \times I$.

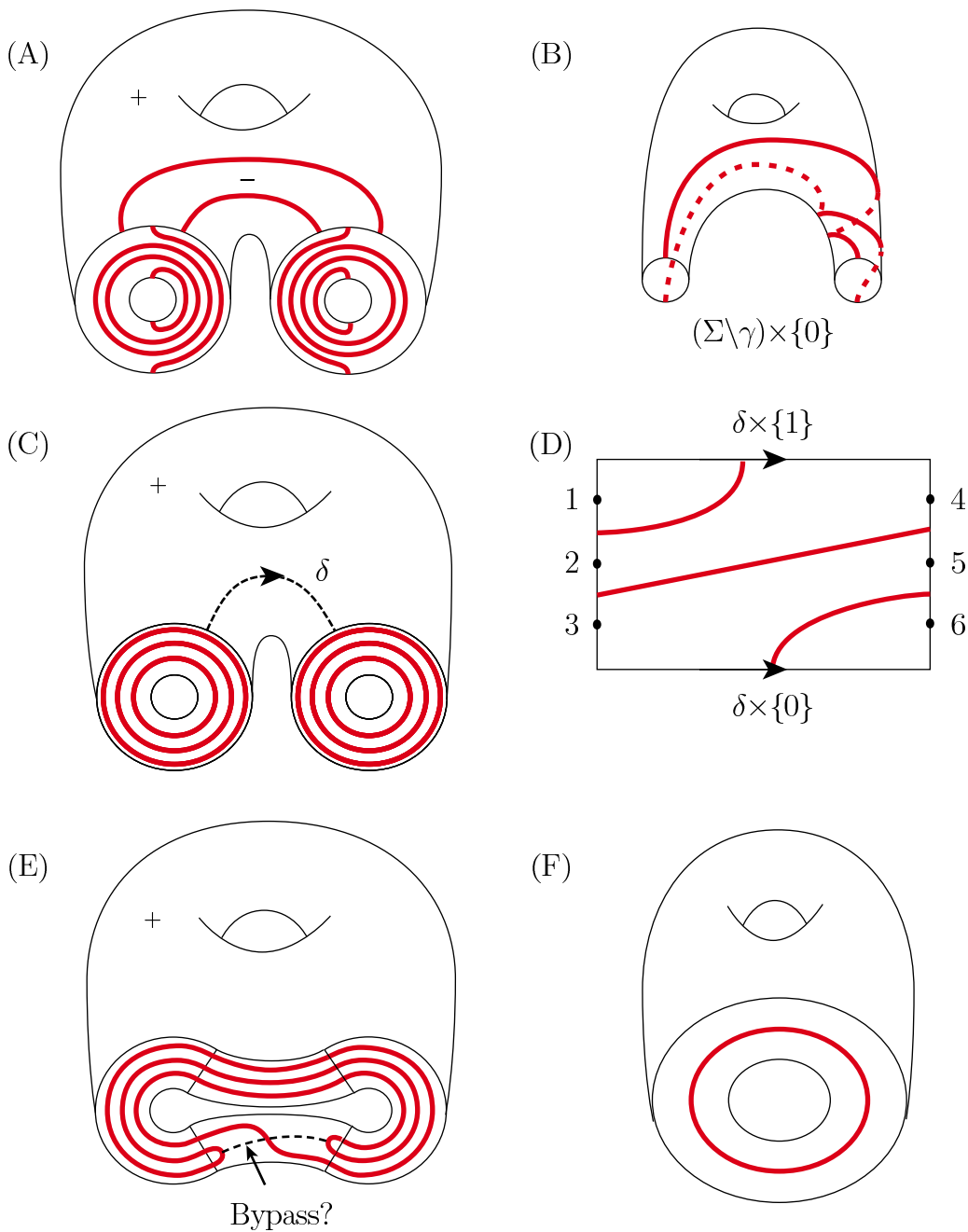
a convex rectangle $\delta \times I$, and again we must consider all possible dividing curve configurations on a splitting convex surface.

Suppose first that the dividing curve configuration on $\delta \times I$ has a boundary-parallel component whose half disk contains the point labelled 2 in $\delta \times I$. (Figure 43(D) shows a different configuration.) This would imply the existence of a bypass with arc of attachment running from 1 to 3. Consider how this bypass is situated relative to $\sigma \times I$ – it crosses two parallel dividing curves and ends on a third curve in Figure 43(A). But a quick computation (Example 11) shows that the effect of pushing $\sigma \times I$ across such a bypass removes both closed dividing curves from $\sigma \times I$, that is, it produces a Type II_0^+ annulus that we had promised to find.

The same logic shows that if any dividing curve is boundary-parallel and centered on the point 3, 4, or 5, a Type II_0^+ can be shown to exist. We are left with the dividing curve configuration of Figure 43(D). The result of cutting along $\delta \times I$ and rounding corners is shown in Figures 43(E,F).

Lemma 1. *There must exist a bypass along the arc of attachment shown in Figure 43(E).*

Sketch of lemma. If such a bypass exists then pushing the vertical annulus of Figure 43(E) through it produces three dividing curves rather than just the one shown in Figure 43(F). One step in a complete proof is arguing that there is a vertical annulus with three dividing curves near the given vertical annulus. This is very similar to the part of the proof of tightness in the toroidal case, shown in Figure 36, in which a more complicated space was shown to exist inside a manifold with a single dividing curve on a vertical annulus in its boundary. In short, the annulus is shown to exist by a folding argument along an isolating curve that is shown to exist near

FIGURE 43. Decomposing $\Sigma \times I$.

the original annulus. This more complicated annulus implies the existence of the desired bypass. \square

Pushing $\delta \times I$ through this bypass produces a new dividing curve configuration on $\delta \times I$ which has boundary-parallel dividing curves centered on the points labelled 3 and 4. As above, this allows us to modify $\gamma \times I$ and produce an annulus of Type II_0^+ .

The rest of the proof of Theorem 9 requires:

- (1) Many other similar reductions.
- (2) Existence of the four types of contact structures must be shown.
- (3) Uniqueness of these contact structures must be established.

We will show the existence and uniqueness of Type II_0^+ tight contact contact structures. Figure 44(A, B) shows $\Sigma \times I$ cut along $\gamma \times I$. Notice that the dividing curves on $\gamma \times I$ are boundary-parallel. The result of rounding corners and the next splitting surface is shown in Figure 44(C). Since $\delta \times I$ intersects only two dividing curves, there is no choice for the diving curve set on $\delta \times I$, it must be the single boundary-parallel arc shown in Figure 44(D). The result of cutting along $\delta \times I$ and rounding corners is shown in Figure 44(E,F). And now the pattern continues, $\epsilon \times I$ intersects dividing curves just twice, and continuing in this fashion we produce a convex decomposition in which all splitting surfaces have boundary-parallel dividing curves, and there is always a unique choice of tight dividing curves.

Thus (2), in this case, follows from Theorem 7, and (3) follows from the forced choice of dividing curves along the way.

It is worth emphasizing that a convex decomposition determines the contact structure near ∂M , near the splitting surfaces, and by uniqueness on all of the resulting B^3 's, that is, a convex decomposition determines the contact structure at every point of M .

This completes the sketch of Theorem 9. \square

The statement of Theorem 9 refers to a choice of dividing curves. This choice can be described explicitly using the notion of a *straddled* dividing curve.

Definition 16. *A dividing curve in $\partial(\Sigma \times I)$ is straddled if there exists a dual convex annulus with a boundary-parallel dividing curve centered on it.*

We record a couple of consequences of Theorem 9 that will be used in applications.

Corollary 1 (Addition). *Let ξ_1 and ξ_2 be tight, non-product contact structures on $\Sigma \times [0, 1]$ and $\Sigma \times [1, 2]$, respectively, that agree on $\Sigma \times \{1\}$. Then $\xi_1 \cup \xi_2$ is tight if and only if no dividing curve on $\Sigma \times \{1\}$ is straddled in both $\Sigma \times [0, 1]$ and $\Sigma \times [1, 2]$. \square*

Corollary 2 (Freedom of Choice). *Let ξ be a non-product tight contact structure on $\Sigma \times I$, and let α_1 and α_2 be a pair of parallel, non-separating curves on Σ . Then there exists a convex embedding of Σ in $\Sigma \times I$ that is isotopic to the inclusion of a boundary component, such that $\Gamma_\Sigma = \alpha_1 \cup \alpha_2$. \square*

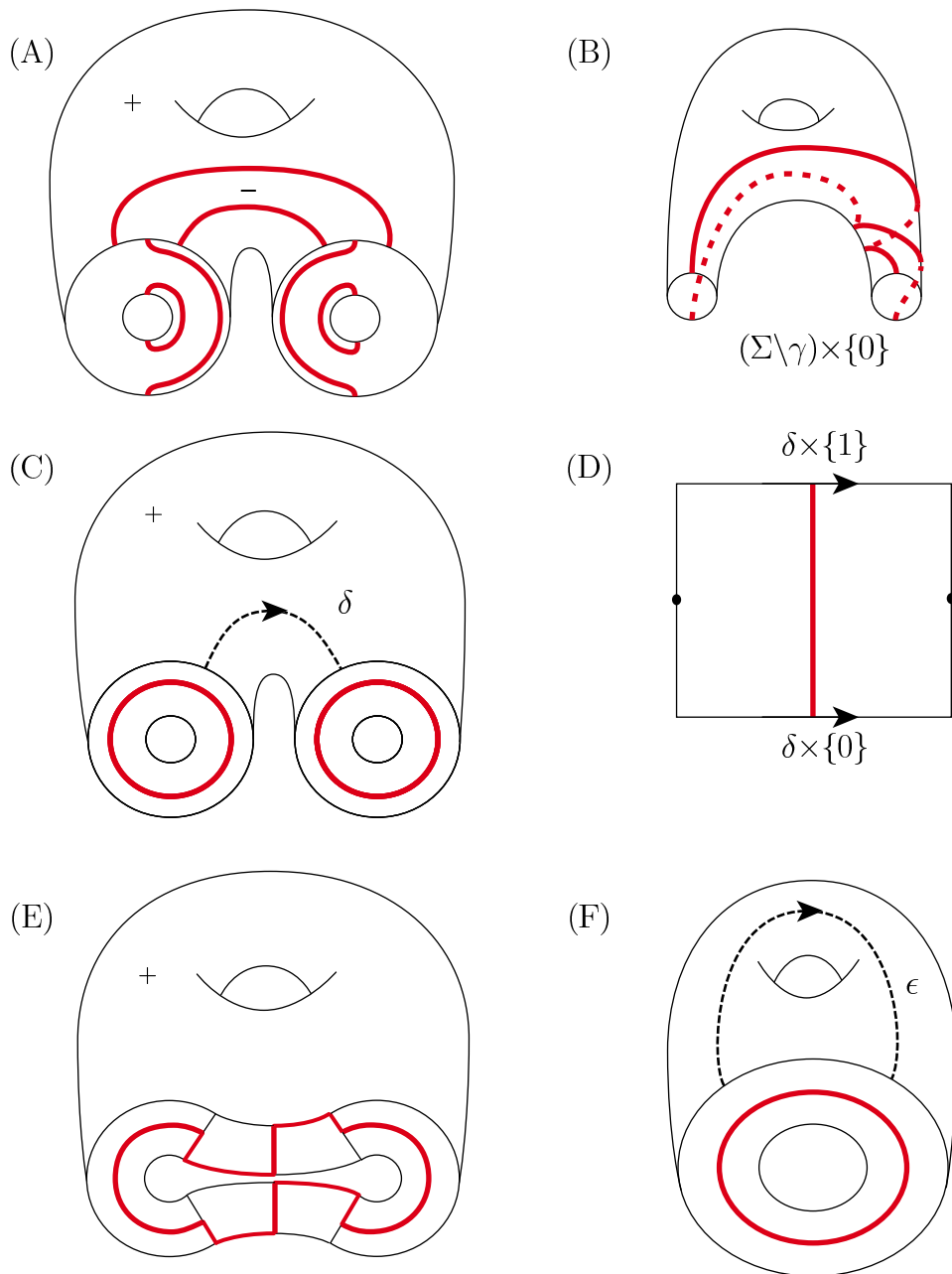


FIGURE 44. Existence of uniqueness of Type II_0^+ .

The next proposition is self-evident and very useful [20].

Proposition 6 (Imbalance Principle). *Let $S^1 \times [0, 1]$ be a properly embedded convex annulus in M such that $S^1 \times \{0\}$ intersects fewer dividing curves than*

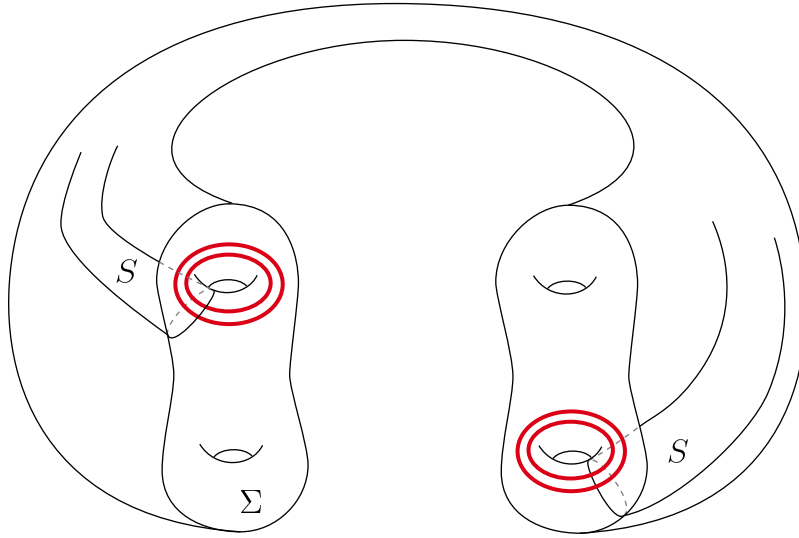


FIGURE 45. The first splitting surface S in $M \setminus \Sigma$.

$S^1 \times \{1\}$. Then $S^1 \times [0, 1]$ contains a bypass centered on a dividing curve intersecting $S^1 \times \{1\}$. \square

Sketch of Theorem 10.

- Given a surface bundle with pseudo-Anosov holonomy φ , pick a fibre, isotop it until it is convex, and cut the bundle along the fibre. The dividing curves on each boundary component consist of a family of parallel pairs of curves.
- If there are more than one pair of parallel curves on either boundary component, then since φ is pseudo-Anosov, there exists an imbalance annulus.
- Isotoping the fibre through the bypass guaranteed by the Imbalance Principle reduces the number of dividing curves. Continue until there is just a single pair on each boundary component.
- By Freedom of Choice a new fibre can be chosen with a fixed pair of non-separating dividing curves.
- Splitting the bundle along this fibre reduces an arbitrary bundle to one of the four standard forms given in Theorem 9. Of the four possible straddlings, two are ruled out because of the tightness of the gluing that recreates the original surface bundle. The other two are related by another application of Freedom of Choice.

\square

Sketch of Theorem 11. By Theorem 6 we may assume M is a closed manifold. Let $\Sigma \subset M$ be a Thurston norm minimizing surface corresponding to a non-zero element of $H_2(M)$ and split M along Σ .

The sutured manifold $M \setminus \Sigma$ has no sutures, but it does have a sutured manifold decomposition. Let the first splitting surface be S , and we shall

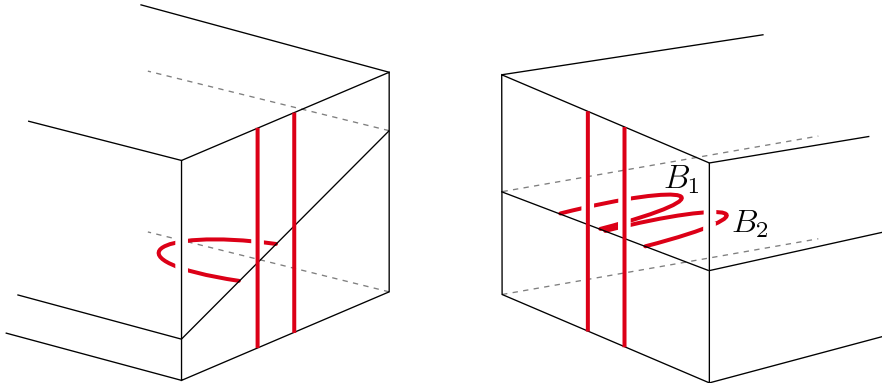


FIGURE 46. Possible location of bypasses before gluing.

assume that S intersects each copy of Σ in a single closed curve as shown in Figure 45. Make $M \setminus \Sigma$ a convex structure by adding a pair of parallel dividing curves dual to ∂S on each boundary component. Make S a convex surface by adding boundary compressible dividing curves σ straddling a component of Γ , the dividing set on the boundary of $M \setminus \Sigma$, on each copy of Σ . If the right curves are straddled, splitting the sutured manifold $M \setminus \Sigma$ along S will correspond to the convex splitting defined by (S, σ) . The remaining steps of the convex decomposition are directly inherited from the sutured manifold decomposition.

This convex decomposition of $(M \setminus \Sigma, \Gamma)$ is by surfaces all of whose dividing curves are boundary-parallel. Thus by Theorem 7, there is a tight contact structure on $M \setminus \Sigma$. Moreover, by construction, one dividing curve on each boundary component of $M \setminus \Sigma$ is straddled by a dividing curve on S .

By Theorem 9 there are four choices of tight contact structure on $\Sigma \times I$ that could be used to attach to $M \setminus \Sigma$ and produce a tight contact structure on M . It should seem very plausible, and it is true, that a curve straddled on both sides gives rise to an overtwisted disk. Thus we insert the unique, non-product, contact structure on $\Sigma \times I$ that gives $(M \setminus \Sigma) \cup \Sigma \times I$ a chance of being tight.

We are two gluing theorems away from a complete proof of tightness on M ; we must glue along each of the boundary components of $\Sigma \times I$. As we have seen, the general form of these gluing proofs is:

- (1) Given an overtwisted disk in M , push Σ off it using bypasses while keeping $M \setminus \Sigma$ tight.
- (2) Analyze which bypasses exist on one component of $M \setminus \Sigma$ and which can be added to the other component while preserving tightness.

Rather than do this in generality, consider the local version of this that is shown in Figure 46. On the left are two dividing curves one of which is straddled. On the right are the two dividing curves about to be identified with the curves on the left. Also shown are two bypasses. The first, B_1 , is

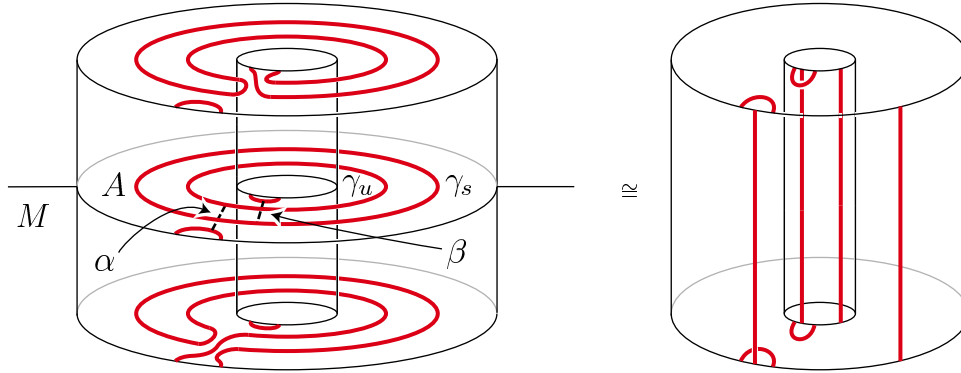


FIGURE 47. Adding a bypass across β is the same as removing a bypass across α .

known to exist by construction, thus if it is removed and added to the other side tightness must be shown to be preserved. The second, B_2 , if added to the left would produce an overtwisted disk, thus, as part of a sufficient gluing theorem, these must be shown not to exist. These local gluing results follow from the next lemma. □

Lemma 2. *Let γ_u and γ_s be a pair of parallel dividing curves on ∂M , and assume γ_s is straddled and the contact structure on M is tight. Then adding a bypass to M across γ_u will produce a tight contact structure.*

Since adding a bypass to M across γ_s produces an overtwisted structure, it follows that γ_u is not straddled.

Proof. Figure 47 shows a neighborhood $A \times I$ of an annular neighborhood A of γ_s and γ_u in ∂M . It also shows the arc of attachment α which straddles γ_s and the arc of attachment β to which a bypass is being added. The annulus parallel and below A shows the result of removing the bypass attached along α , and the annulus above A shows the result of adding a bypass along β . The figure on the right shows the dividing curves on the boundary $A \times I$.

At least on the boundary, the figure on the right looks like a product contact structure on $A \times I$, and indeed it is. Since the attaching curves, α and β , are disjoint, the contact structure on A can be built by first attaching a bypass to the bottom annulus along β and then attaching a bypass along α . From this point of view, the isotopy class of the dividing curves remains unchanged after adding each bypass (see also Example 13), and thus the contact structure is a product. It now follows that adding a bypass across β is the same as removing a bypass in M attached along α , and this operation preserves tightness. □

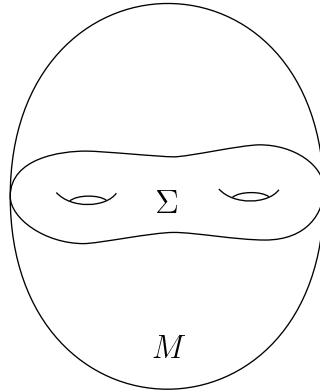


FIGURE 48. Haken homology sphere.

6. OPEN QUESTIONS

There are two fundamental classes of open questions:

- (1) Which M^3 carry tight contact structures?
- (2) What are the topological implications of carrying a tight contact structure?

The central existence question, particularly from the point of view developed in this paper, is the question of whether or not Haken homology spheres M always carry tight contact structures.

In such a manifold, every surface $\Sigma \subset M$ must separate. In particular if there is a tight contact structure ξ on M , then $e(\xi)(\Sigma) = 0$. This means that if Σ is convex, then $\chi(R_+) = \chi(R_-)$. This is exactly opposite to the extremal case when $\chi(R_+) = \chi(\Sigma)$ and $\chi(R_-) = 0$.

Presumably constructing contact structures will involve:

- Classification of such structures on $\Sigma \times I$ and
- new gluing theorems.

Example 18. *Perhaps the simplest example of this sort of classification question on $\Sigma \times I$ is shown in Figure 49. Preliminary work of Cofer [6] shows there is exactly one tight, non-product, contact structure with these dividing curves. This example has the bizarre property that if you add any non-trivial bypass, it becomes overtwisted. It follows that it does not occur as a subset of any tight contact structure on $\Sigma \times I$ other than itself, and it may not show up in any tight closed 3-manifold.*

Very little is known about (2), implications of carrying a tight contact structure, so we will describe results that have been obtained in lamination theory, that perhaps have analogues in contact topology.

Definition 17. *A lamination of M^3 is a disjoint union of surfaces which are locally homeomorphic to the product of D^2 and a closed subset of I .*

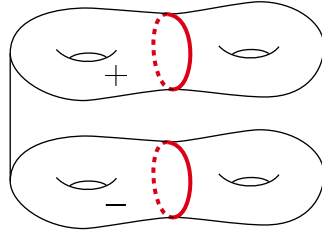


FIGURE 49. A non-extremal boundary configuration.

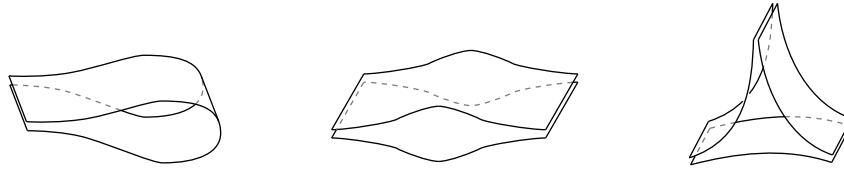


FIGURE 50. Complementary regions of a general lamination.

A lamination is essential if the leaves are incompressible, the complementary regions are irreducible, and there are no folded leaves.

A lamination is genuine if it is essential and some complementary region is not a product of a boundary leaf and I .

Figure 50 shows, in order, a folded leaf, a complementary region that is a product of a boundary leaf and I , and a complementary region that is not such a product.

Definition 18. *The Euler characteristic of a surface with cusped boundary is defined to be the usual Euler characteristic of the underlying space minus half of the number of cusps.*

The cross-sections of the complementary regions shown in Figure 50 are a disk with one cusp ($\chi = 1/2$), a disk with two cusps ($\chi = 0$), and a disk with three cusps ($\chi = -1/2$). The definition of essential consists of bans on various types of positive Euler characteristic, while the notion of a genuine lamination postulates the existence of some negative Euler characteristic in M . We shall see that atoroidal manifolds are group negatively curved (Theorem 13). It is not clear what additional structure should be made for contact structures that might make the this theorem apply in that setting as well.

By the JSJ decomposition theorem, there is a unique I -bundle structure \mathcal{I} on the ends of each complementary region. Thus each complementary region decomposes as the union of a \mathcal{I} and the guts \mathcal{G} as shown in Figure 51.

The key features of this decomposition are:

- \mathcal{G} is compact.

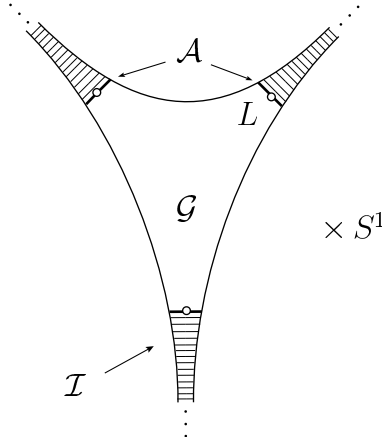


FIGURE 51. Structure on the complementary region of a genuine lamination.

- By maximality of \mathcal{I} , \mathcal{G} has no *product disks*, that is, there are no non-trivial rectangles in \mathcal{G} with sides that alternately consist of I -bundle fibres of \mathcal{I} and arcs in leaves of the lamination.
- An essential lamination is genuine if and only if $\mathcal{G} \neq \emptyset$.
- $\mathcal{G} \cap \mathcal{I}$ is a finite union of annuli \mathcal{A} . The union of the cores of these annuli are a link denoted L .

Definition 19. M is group negatively curved if there exists a constant C such that for every null-homotopic curve, $f : S^1 \rightarrow M$, there exists an extension of f to a disk D such that

$$\text{area}(f(D)) < C \cdot \text{length}(f(\partial D)).$$

M is group negatively curved with respect to a link L in M if there exists a constant C such that for every null-homotopic curve $f : S^1 \rightarrow M$, there exists an extension of f to a disk D such that

$$\text{area}(f(D)) < C \cdot (\text{length}(f(\partial D)) + \text{wr}(f(\partial D), L)).$$

The wrapping number $\text{wr}(f(\partial D), L)$ is a geometric linking number and is defined to be the minimum, taken over all disks E with $\partial E = f(\partial D)$ of the number of points of intersection of E with L .

The inequality in the definition of *group negatively curved with respect to a link L in M* is equivalent to the existence of a constant such that at least one of the two inequalities is satisfied:

$$\text{area}(f(D)) < 2C \cdot \text{length}(f(\partial D))$$

or

$$\text{area}(f(D)) < 2C \cdot \text{wr}(f(\partial D), L).$$

We will need the following remarkable theorem.

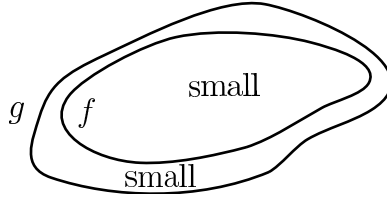


FIGURE 52. A small area homotopy that doesn't increase length much.

Theorem 12. (Gabai's Ubiquity Theorem [15]) *If M is closed, irreducible, and atoroidal, and if $L \not\subset B^3$, then M is group negatively curved with respect to L .* \square

Theorem 13. [17] *If M is atoroidal and contains a genuine lamination λ , then M is group negatively curved.*

Before applying Gabai's Ubiquity Theorem to the proof of this, we will need the following lemma which says that to prove an isoperimetric inequality for all null-homotopic curves, it is enough to prove the inequality on a "dense" subset.

Lemma 3. *Let A be the set of all null-homotopic curves $g : S^1 \rightarrow M$, and let S be a subset of A . If*

- *all $f \in S$ satisfy an isoperimetric inequality,*
- *each $g \in A$ is approximated by an $f \in S$ by a small area homotopy, and*
- *length(f) is not drastically longer than length(g),*

then all $g \in A$ satisfy an isoperimetric inequality.

Proof. This follows by piecing together the homotopies shown in Figure 52. \square

Sketch of Theorem 13. To apply this lemma think of \mathcal{G} as a big, fat subset of M . Then to show M is group negatively curved, it is enough to prove an isoperimetric inequality for the set of null-homotopic curves $f : S^1 \rightarrow M$ such that

- (1) f is transverse to λ .
- (2) Each component of $f^{-1}(\mathcal{G})$ has length greater than some constant ε .

In other words, short bits of $f^{-1}(\mathcal{G})$ can be efficiently removed as in Figure 53.

Given such a null-homotopic $f : S^1 \rightarrow M$, there is, by Theorem 12, a disk of null-homotopy, D , such that

$$\text{area}(f(D)) < 2C \cdot |f(D) \cap L|.$$

Thus it will be enough to show that for some constant C'

$$2C \cdot |f(D) \cap L| < C' \cdot \text{length}(\partial f(D)).$$

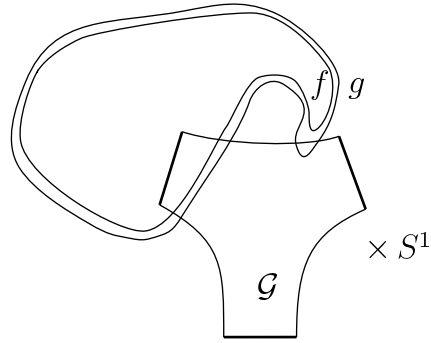


FIGURE 53. Short portions of $g^{-1}(\mathcal{G})$ can be removed efficiently.

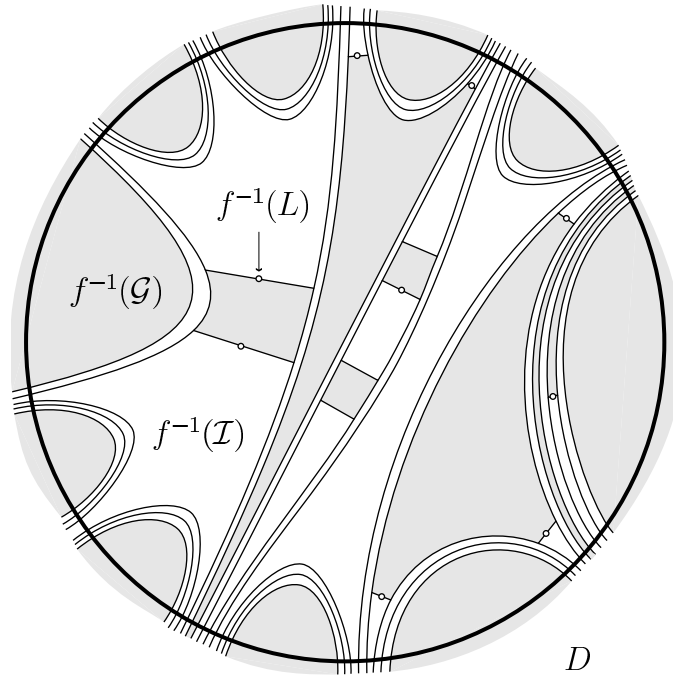


FIGURE 54. The pullback of λ , \mathcal{G} , and \mathcal{I} to D .

Figure 54 shows $f^{-1}(D)$. The figure shows $f^{-1}(\mathcal{G})$ as shaded, and $f^{-1}(\mathcal{I})$ as white. Since we are only trying to give a sketch of the main ideas, we will think of f as an embedding.

Figure 55 shows regions that might occur as subsets of $f^{-1}(D)$. The first region, a null-homotopic circle, can be removed by choosing a new map of $D \rightarrow M$ since leaves of λ are incompressible. The second region, a folded leaf, can not occur in an essential lamination. And finally the third region, a half disk mapped into \mathcal{G} does occur, and thus we arrive at

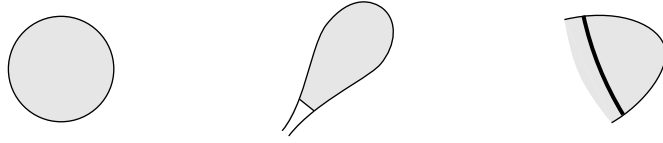


FIGURE 55. Possible regions of D with positive Euler characteristic.

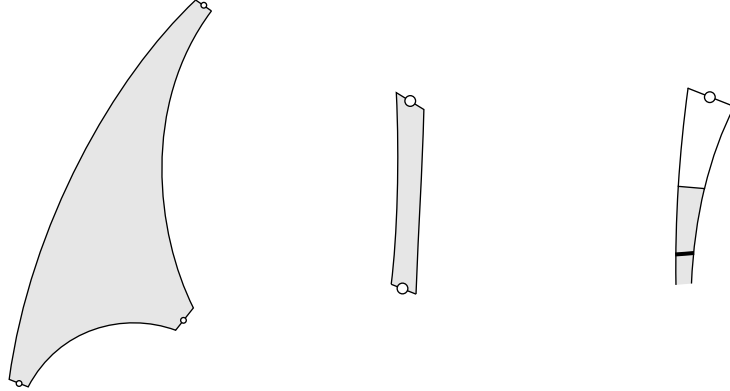


FIGURE 56. Regions of D which contain points of $f^{-1}(L)$.

Conclusion 1. Regions of $f^{-1}(D)$ with positive Euler characteristic contribute at least ε to the length $f(\partial D)$.

Figure 56 shows typical regions of $f^{-1}(D)$ which contain points of $f^{-1}(L)$. The first figure, a cusped triangle, has negative Euler characteristic. The second region shown has Euler characteristic zero and is a product disk in \mathcal{G} . This can not exist by the definition of \mathcal{G} . The third region also has Euler characteristic zero, but it contains an arc that is mapped into \mathcal{G} , thus it contributes at least ε to $\text{length}(f(\partial D))$. After removing the middle regions that can not exist we reach

Conclusion 2. Points of $f^{-1}(L)$ either show up in regions of negative Euler characteristic or they contribute at least ε to $\text{length}(f(\partial D))$.

We can now complete the proof. We have a disk D such that

$$\text{area}(f(D)) < 2C \cdot |f(D) \cap L|,$$

thus a large area disk gives many points of $f^{-1}(L)$. By Conclusion 2, these points either directly contribute to the length of $f(\partial D)$, or they show up in regions of negative Euler characteristic. But $\chi(D) = 1$, thus the existence of regions with negative Euler characteristic implies the existence of regions with positive Euler characteristic. By Conclusion 1, these in turn contribute even more to the length of $f(\partial D)$. Thus we conclude

$$\text{area}(f(D)) < 2C \cdot |f(D) \cap L| < C' \cdot \text{length}(f(\partial D)).$$

□

A key feature of this proof that doesn't have an obvious analogue in contact topology is the crude notion of length given by pulling back \mathcal{G} to ∂D .

We would like to end up by pointing out that there are not clear connections between tight contact structures on M and the fundamental group of M . For instance, it is not known if a homotopy 3-sphere supports a tight contact structure whether it must be S^3 .

By way of contrast, there are many $\pi_1(M)$ actions that can be constructed from foliations and laminations. The *leaf space* is the quotient of the universal cover by leaves and complementary regions. The quotient is an *order tree*, and there is always an action of $\pi_1(M)$ on it.

Bestvina and Mess [2] show that if M is group negatively curved then there is an action of $\pi_1(M)$ on S^2 . This can be applied to the manifolds of Theorem 13, and indeed by Calegari's work [3], there are far more manifolds in this collection than originally realized.

Palmeira's Theorem [27] is generalized to laminations in [16], and it follows that the universal cover $(\tilde{M}, \tilde{\lambda})$ is always homeomorphic to a product $(\mathbb{R}^2, \kappa) \times \mathbb{R}$ where κ is a lamination of the plane. Calegari and Dunfield [5] point out that (\mathbb{R}^2, κ) can be thought of as (\mathbb{H}^2, κ) and from this they can sometimes produce an action on S_∞^1 .

Calegari and Dunfield [5] have more general results. They generalize Thurston's work on the universal circle, and using Candel's theorem [4], they identify leaves of λ with \mathbb{H}^2 , and they identify all S_∞^1 's coming from the \mathbb{H}^2 's to get a $\pi_1(M)$ action on S_{univ}^1 . This works for taut foliations and some genuine laminations.

Acknowledgements. This article is based on a series of talks given at the Tokyo Institute of Technology from June 3–7, 2002. I would like to thank Professor Matsumoto for inviting me and Professor Kojima for hosting my visit. I would particularly like to thank Ko Honda for his lectures during an informal seminar at the University of Georgia that introduced me to his point of view in contact topology and for suggesting many improvements to this paper.

REFERENCES

- [1] D. Bennequin, *Entrelacements et équations de Pfaff*, Astérisque **107–108** (1983), pp. 87–161.
- [2] M. Bestvina, G. Mess, *The boundary of negatively curved groups*, J. Amer. Math. Soc., **4** (1991), no.3, pp. 469–481.
- [3] D. Calegari, *The geometry of \mathbb{R} -covered foliations*, Geom. Topol., **4** (2000), pp. 457–515.
- [4] A. Candel, *Uniformization of surface laminations*, Ann. Sci. École Norm. Sup. (4) **26** (1993), no. 4, pp. 489–516.
- [5] D. Calegari, N. Dunfield, *Laminations and groups of homeomorphisms of the circle*, to appear in Invent. Math. (2002)
- [6] T. Cofer, Ph.D. thesis, University of Georgia, (2002) in preparation.

- [7] V. Colin, *Recollement de variétés de contact tendues*, Bull. Soc. Math. France **127** (1999), no. 1, 43–69.
- [8] V. Colin, *Sur la torsion des structures de contact tendues*, to appear in Ann. Sci. Éc. Norm. Sup.(4) **34** (2001), no. 2, pp.267–286.
- [9] V. Colin, *Une infinité de structures de contact tendues sur les variétés toroïodales*, Comment. Math. Helv. **76** (2001), pp. 353–372.
- [10] V. Colin, E. Giroux and K. Honda, *On the coarse classification of tight contact structures*, (preprint)
- [11] Y. Eliashberg, *Classification of overtwisted contact structures on 3-manifolds*, Invent. Math. **98** (1989), pp. 623–637.
- [12] Y. Eliashberg, *Contact 3-manifolds twenty years since J. Martinet’s work*, Ann. Inst. Fourier **42** (1992), pp. 165–192.
- [13] Y. Eliashberg and W. Thurston, *Confoliations*, University Lecture Series **13**, Amer. Math. Soc., Providence (1998).
- [14] D. Gabai, *Foliations and the topology of 3-manifolds*, J. Diff. Geom. **18** (1983), pp. 445–503.
- [15] D. Gabai, *Quasi-minimal semi-Euclidean laminations in 3-manifolds*, Surveys in differential geometry, Vol.III Cambridge, MA, 1996), pp. 195–242, *Int. Press. Boston, MA, 1998*.
- [16] D. Gabai, W. Kazez, *Homotopy, isotopy and genuine laminations of 3-manifolds*, Geometric Topology, vol. 1, *AMS/IP* (1997), pp. 123–138.
- [17] D. Gabai, W. Kazez, *Group negative curvature for 3-manifolds with genuine laminations*, Geom. Topol. **2** (1998), pp. 65–77.
- [18] E. Giroux, *Convexité en topologie de contact*, Comment. Math. Helv. **66** (1991), pp. 637–677.
- [19] E. Giroux, *Structures de contact sur les variétés fibrées en cercles au-dessus d’une surface*, Comment. Math. Helv. **76** (2001), no. 2, pp. 218–262.
- [20] K. Honda, *On the classification of tight contact structures I*, Geom. Topol. **4** (2000), pp. 309–368.
- [21] K. Honda, *Gluing tight contact structures*, to appear in Duke Math. J.
- [22] K. Honda, W. Kazez and G. Matić, *Convex decomposition theory*, Internat. Math. Res. Notices (2002), 55–88.
- [23] K. Honda, W. Kazez and G. Matić, *Tight contact structures on fibered hyperbolic 3-manifolds*, (2001) preprint.
- [24] K. Honda, W. Kazez and G. Matić, *On the Gabai-Eliashberg-Thurston Theorem*, (2001) preprint.
- [25] Y. Kanda, *The classification of tight contact structures on the 3-torus*, Comm. in Anal. and Geom. **5** (1997), pp. 413–438.
- [26] S. Makar-Limanov, *Tight contact structures on solid tori*, Trans. Amer. Math. Soc. **350** (1998), pp. 1013–1044.
- [27] C. Palmeira, *Open manifolds foliated by planes*, Ann. Math. (2) **107** (1978), no. 1, pp. 109–131.
- [28] W. Thurston, *A norm for the homology of 3-manifolds*, Mem. Amer. Math. Soc. **59** No. 339, (1986), pp. 99–130.

UNIVERSITY OF GEORGIA, ATHENS, GA 30602

E-mail address: will@math.uga.edu

URL: <http://www.math.uga.edu/~will>